Solid Oxide Electrolyzer Cell Modeling: A Review

Jan Pawel Stempien[a,b], Qiang Sun[c], Siew Hwa Chan[*,a,b]

[a]*School of Mechanical & Aerospace Engineering, Nanyang Technological University (NTU)*
50 Nanyang Avenue, Singapore 639798, Singapore

[b]*Energy Research Institute at NTU, Nanyang Technological University*
1 CleanTech Loop #06-04, Singapore 637141, Singapore

[c]*Department of Advanced Materials and Nanotechnology, College of Engineering, Peking University*
Beijing 100871, China

Abstract

Solid Oxide Electrolyzer Cell (SOEC) is a very good candidate technology for securing sustainable development for the future. It allows CO_2 to be recycled into usable fuels and has potential for hydrogen economy. In this work the authors focus on development of SOEC through modeling different aspects of the cell: from design of specific elements to final incorporation of electrolyzers in the global energy system and network. The publications reviewed span from the 1970s to the present day and cover a selection of most contributed works. The selected publications provide means for modeling the solid oxide electrolyzer cell in both steady and transient states. The scale of the models ranges from micro to macro and to global energy system levels. The thrust of this work is to summarize the current level of development in modeling the solid oxide electrolyzer cell and to highlight unresolved problems and provide pointers in terms of research gaps requiring closer attention by engineers and scientists.

Keywords: Solid Oxide Electrolyzer Cell (SOEC), Modeling of Solid Oxide Electrolyzer, Review of SOEC modeling, electrolysis

1. Introduction

Electrolysis is historically known as an electrochemical process for splitting water into hydrogen and oxygen. Chemically it can be written as

$$2H_2O \rightarrow 2H_2 + O_2$$
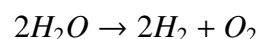
The history of water electrolysis dates back to the 1800s and the discovery of electric water splitting by

Nicholson and Carlisle [1]. A good review can be found in section 7 of Zeng and Zhang's review on alkaline water electrolysis [2]; here it is presented in brief. It took more than a century from that stage to commercially develop the first electrolysis technology. During that time Faraday's law was developed [3], the Nernst equation was derived [4] and the general science of electrochemistry was established [5]. The early 20th century brought the first big scale applications of hydrogen production and definition of the classical methods of electrolysis. In the second half of the 20th century the first proton exchange membrane and solid oxide electrolyz-

---

[*]Corresponding author

Email addresses: jan2@e.ntu.edu.sg (Jan Pawel Stempien[a,b]), sunqiang@pku.edu.cn (Qiang Sun[c]), mshchan@ntu.edu.sg (Siew Hwa Chan[*,a,b])

ers were developed. Now, water splitting technologies include photoelectrolysis [6], thermolysis [7], thermochemical processes [8] and biological processes [9, 10]. Shortly after the first large scale electrolysis plants were built, another option for the production of hydrogen came to light, based on coal gasification and methane reforming. Currently, most of the world's hydrogen is produced through methane reforming [11], as it is the cheapest large-scale production technology. The use of electrolysis for hydrogen production made a brief return to the scientific spotlight after the oil shocks in 1970s [12]. Now, it is having another period of opportunity due to growing environmental concerns and the availability of renewable energy [13, 14]. The main interest at present for future hydrogen generation is in alkaline, Polymer Exchange Membrane and Solid Oxide electrolyzers.

Alkaline electrolysis is the oldest and only commercially available technology. For each electrolyzer cell, there are two electrodes, one positive and one negative, and an electrolyte sandwiched in between. In the case of alkaline electrolyzer with electrodes made of metals, most commonly Ni, Co, Fe or Pt/C, the electrolyte would be liquid KOH and the two electrolyzer chambers are divided by a diaphragm (e.g. NiO). This technology is the most energy intensive one and produces hydrogen of the lowest purity. A good review of the development of this technology can be found in ref. [2].

Polymer exchange membrane (PEM) electrolyzers, or as they are often called solid polymer electrolyzers (SPE) are based on reversed PEM fuel cell technology. They can operate at the same temperature as alkaline electrolyzers or higher (in the case of high-temperature PEM) and generally enjoy better efficiency. They are about to become commercially available in the near future. PEM electrolyzers can be viewed as an incremental development of alkaline electrolyzers. The main difference is that they use a more advanced diaphragm (i.e., polymer membrane). A good review of the development of this technology can be found in ref. [15].

Solid Oxide Electrolyzers are the least commercially developed technology. They operate at much higher temperatures than the other technologies, and consume much less electricity due to superior en-

ergy conversion efficiency. However, due to high-temperature operation, special materials are required to withstand the conditions of the process. As regards the plant, there are no promising products available that provide long-term hassle-free operation of the accessories. The technology, besides offering the highest faradic efficiency, also offers a possibility of direct electrolyzing of CO_2. Apart from that, the technology can extend to co-electrolyzing H_2O and CO_2 simultaneously. The product of such co-electrolysis is syngas, which can then be re-processed to yield synthetic fuel [16–18]. For this reason, solid oxide electrolyzers offer the possibility of chemical energy storage/carrier when converting renewable energy or excess energy from fossil power plants to hydrogen or syngas. This also provides the rationale for writing this review paper. To the best knowledge of the authors, there is no available review effort concentrating solely on modeling the Solid Oxide Electrolyzer Cell. A good review of recent development of this technology can be found in ref. [19, 20].

2. Broader context

Environmental concerns over the past few years have grown to become one of the most important factors driving research and development efforts. One major area where environmental consciousness is exhibited is in the field of energy. For years it has been one of the biggest contributors to emissions of sulfur oxides (SO_x), nitrogen oxides (NO_x), heavy metals and carbon dioxide. Engineers and scientists have managed to reduce emissions significantly [21–23], but not CO_2 [24]. It may seem now that the only way to succeed in transforming the energy production sector is by a complete restructuring of existing production. Several solutions are being implemented to tackle rising emissions [25–29], with renewable energy sources being one of the most popular options. Nevertheless, electricity needs to be produced in amounts that exactly match instantaneous requirements, and thus intermittent renewable energy is not the solution, at least not at the present time [30, 31].

There is, however, an alternative to the direct use of renewable energy resources. Solid Oxide Cells (SOCs) are devices that are capable of transforming
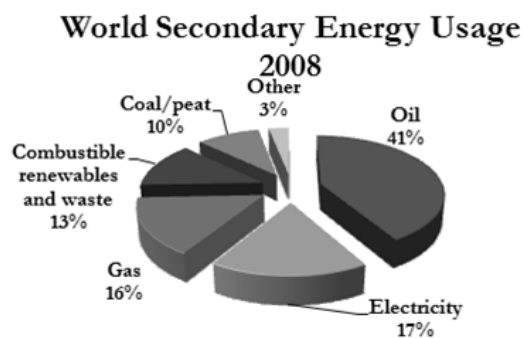
Figure 1: Total secondary energy consumption by source [33]

Figure 2: Schematic of a Solid Oxide Electrolyzer cell in a planar configuration, with air as a sweep gas and steam as a reactant. The basic reactions on the electrodes and the component nomenclature is given

one form of energy to another in a highly efficient and environmentally benign way [32]. In the fuel cell mode of operation they produce electricity from hydrogen, carbon monoxide or reformed hydrocarbons (SOFC), while in the electrolyzer mode they convert electricity into chemical energy of the chosen fuel. SOCs have been proposed to operate in terrestrial and space applications, revitalizing the artificial atmosphere, powering cars or producing electricity. More recently, they were proposed to work as hydrogen or synthetic fuel production systems [17].

Fossil fuels are the most widely used form of energy, and gas and oil made up over 57% of secondary energy use, while electricity only 17% (Figure 1) [33]. It would be unwise to abandon existing infrastructure for gas and oil, especially when syngas (H_2 and CO) can be co-electrolyzed from water vapor and CO_2 in combustion products [34]. This situation provides a great opportunity for the development of solid oxide cells as a bridge technology. Eventually, carbon can be excluded from the loop by moving to hydrogen only [35, 36]. A report showed that presently 96% of hydrogen gas is produced from fossil fuels [37], which is without doubt environmentally unfriendly. Among possible ways of achieving sustainable production of hydrogen, i.e. electrolysis, thermo-chemical processes, thermolysis, photoelectrolysis, etc., SOC technology is considered to be the cheapest and most efficient technology [17].

3. Solid Oxide Electrolyzer Cell models

Solid Oxide Electrolysis Cell (SOEC) or Solid Oxide Steam Electrolyzer (SOSE) (Figure 2) is an electrochemical energy conversion cell, which transforms electrical energy from passing electrons to chemical energy of a fuel. SOEC is capable of producing carbon monoxide, hydrogen and a mixture of both by electrochemical reactions. It continues to deliver the fuel as long as steam and/or carbon dioxide and electrical energy are supplied.

In reality the lifespan of a cell is limited by the degrading of its components. A typical SOEC is based on a pure ionic conductor in the form of a solid electrolyte. The most commonly used one is the Yttrium-Stabilized Zirconia (YSZ), which allows the transporting of oxygen ions when polarized with an electrical field. There are also other, less popular kinds of SOEC, i.e. co-ionic cells and proton conducting cells, where both oxygen and hydrogen ions or only hydrogen ions are transported through the membrane. This study is limited to oxygen ion conducting cells (not necessarily based on YSZ). The solid electrolyte is sandwiched in between two electrically connected porous electrodes and creates a closed electrical circuit. Beside the positive electrode-electrolyte-negative electrode (PEN) assembly, each complete cell consists of interconnects and gas channels. The present design of the cell exactly mirrors the structure of a solid oxide fuel cell, thus a detailed description of SOEC structure is excluded from this study and interested readers can refer to ref. [31] for details. It is worth mentioning
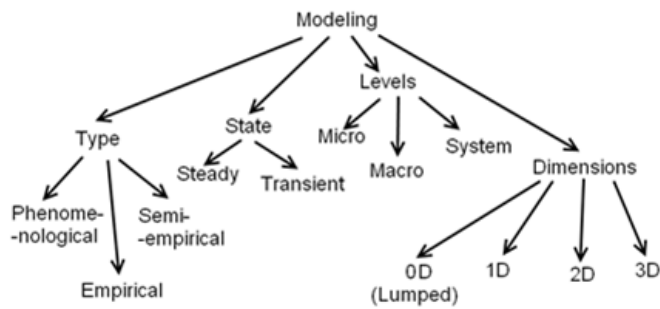
Figure 3: Categories of models of physical phenomena
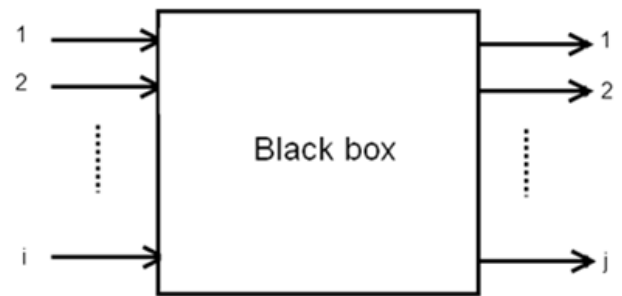
Figure 4: Inputs and outputs of the black box model

that since SOEC is made of solid components, it is in principle possible to shape it to any desired specifications.

Like SOFC, electrolysis cells can be connected in series to form a stack. SOEC shares design flexibility and high operational efficiency with SOFC. The current degree of cell development allows the same cell to be operated in SOEC or SOFC mode within a certain polarization range. This offers interesting possibilities for application of the Solid Oxide Cell (SOC) to shape the energy landscape.

Operation of SOEC, complicated as it is, is relatively easy to explain. On the cathode side of the cell (fuel electrode), steam and/or carbon dioxide are/is delivered, gases pass through the porous electrode and reach the triple phase boundary where reactions and charge transfer occur, thus splitting to hydrogen and/or carbon monoxide, while oxygen ions are pumped to the anode side of the cell (oxygen electrode) through the electrolyte. A Faradic reaction splits anions to electrons and oxygen molecules. Oxygen gas diffuses to the anode gas chamber, while electrons pass through the external circuit and inject into the cathode, thus closing the circuit. If a cell is operated at a high enough voltage, it produces both heat and chemical fuel(s). A typical SOEC operates in a temperature range of 450°C–1000°C at atmospheric or elevated pressures [32].

3.1. Modeling

Modeling of any physical process can be done in several ways (Figure 3) depending on the purpose of the simulation. One of the basic distinctions is between empirical and phenomenological modeling. Empirical modeling has developed in step

with the rise of computing capabilities. It does not require a full understanding of the physics behind the process. It is even possible to model a physical process/system without having any knowledge of it. Models of this kind are called "black boxes", and they are based on artificial intelligence, genetic programming, etc. The process or device is recognized literally as a box with i-th number of inputs and j-th number of outputs (Figure 4). Large amounts of experimental data are required to calibrate the models. Phenomenological models, on the other hand, are based on the laws of physics and they provide a good explanation of why the process behaves the way it does. All of the parameters in models of this type have a physical meaning, unlike in empirical or semi-empirical models.

Due to the lack of properties of the materials, combinations of both models are used (gray box models). To the best knowledge of the authors, no pure empirical model of SOEC has been developed to date. It is worth mentioning that there are a few empirical models of SOFC available in the literature [33, 38]. Nevertheless, they did not gain any popularity, probably due to the lack of sufficient input to understand the phenomena entirely.

A modeling study in the early stages is usually in steady state, meaning time independent. These models are used to predict performance and to optimize the operating and design parameters of an SOEC. Transient, time dependent models are useful for understanding the actual operation, including safety considerations, determining the control strategy and responding to an external load (output of

fuel) demand.

Another way to differentiate the models is by scale. When energy scale is being considered at a system level, then the SOEC is simply one part of a complex thermodynamic system. If optimization is conducted at a component level, then macro- or micro-scale models are used. Available literature is either on one or the other scale. There is generally no universal model combining two or more scales, thus giving rise to speculation on a more realistic performance of a SOEC working in real conditions, which may be far from the experimental conditions (i.e. high vs. low chemicals conversion).

When system level modeling is considered, SOEC electrochemistry is usually assumed to be constant over the simulated range and the power response of the cell is modeled by one linear equation associating voltage with current. In general, performance of a cell is fixed and independent of operating conditions. Such models can only be used for basic feasibility studies.

Macro- and micro-level models are much more sophisticated. In the micro-level simulations, sophisticated statistical tools are used to assess the performance of cermet electrodes. The macro-level models are between the system- and the micro- levels in terms of complexity and they are the most commonly used. They provide a decent trade-off between the choice of control parameters and the computational cost.

The last distinction between the models is by the number of analyzed dimensions. This division can be associated with the previous one, i.e., system-level models are usually zero dimensional, macro-level models can be 1D, 2D or 3D, and micro-level models are often 1D or 2D. In general, the lower the number of dimensions involved, the faster the computation will be. Considering the geometry of the cell, one might easily notice that one of the dimensions, i.e., the thickness of the cell is much smaller than all the others. Therefore one-dimensional models should be more effective for cell modeling. Three dimensional models are usually adopted for the stack configuration design.

The vast majority of available models are focused on predicting the electrical performance of the cell, fuel conversion and output and cell/system effi-ciency, thus are electrochemistry based.

It is generally advised to become acquainted with a review paper or book on SOFC modeling [31, 39] before approaching this work.

3.2. Theory

The performance of a Solid Oxide Electrolysis Cell depends largely on the reaction rates occurring at the triple phase boundary, operating temperature and pressure, supply of electricity, microstructure of the cell, among others. The net reactions for the cathode are:

$$
\begin{aligned}
H_2O\,(g) + 2e^- &\rightarrow H_2\,(g) + O^= \\
CO_2\,(g) + 2e^- &\rightarrow CO\,(g) + O^=
\end{aligned}
\tag{1}
$$

For the anode:

$$
O^= \rightarrow {}^1/_2 O_2 + 2e^-
\tag{2}
$$
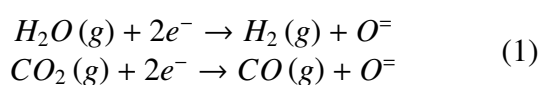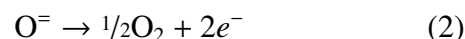
The overall reaction becomes:

$$
H_2O + CO_2 \rightarrow H_2 + CO + O_2
\tag{3}
$$
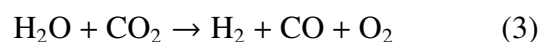
With reference to the electrolyte process mechanism, the reactions can be written in the following manner. For the fuel electrode (the cathode):

$$
\begin{aligned}
H_2O(g) + 2e^- + V_o^{\bullet\bullet} &\rightarrow H_2(g) + O_o^x \\
CO_2(g) + 2e^- + V_o^{\bullet\bullet} &\rightarrow CO(g) + O_o^x
\end{aligned}
\tag{4}
$$
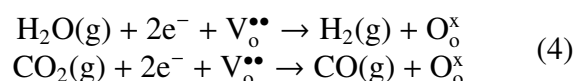
For the air electrode (the anode):

$$
O_o^x + 2h^\bullet = {}^1/_2 O_2(g) + V_o^{\bullet\bullet}
\tag{5}
$$
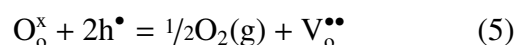
For the electron—electron hole pair:

$$
2\,(e^- + h^\bullet) \longleftrightarrow 0
\tag{6}
$$

Real reaction mechanisms are complex and still not well understood, thus the above reactions are used for simplicity. The reaction rate depends on temperature, pressure, concentration of products, time in the reaction zone and the catalyst used. Unfortunately, the models developed to date omit considerations of the kinetics of reaction, mostly due to a lack of kinetic data and complicated patterns of the reactions that occur. The problem of limited knowledge of the reaction path is omitted in developed models by the simple assumption that the reaction is instantaneous and conversion is either assumed or

is fitted to match experimental data. The approach is taken from the modeling of fuel cells, where the hydrogen reduction reaction is close to instantaneous. However, oxygen evolution reactions require larger energy inputs, and are kinetically slow. Moreover, such models are unable to predict the performance of a cell in conditions which have not been investigated experimentally.

Limiting processes involved in cell operation include:

- Porous Gas Diffusion

- Adsorption/Desorption

- Surface Diffusion

- Reaction Kinetics

- Charge Transfer

- Electrolyte Transport

These processes, excluding adsorption/desorption, surface diffusion and reaction kinetics, are usually modeled with Butler-Volmer equation, Ohm's law, Faraday's law and one of the several gas transport laws.

Modeling of a SOEC focuses on predicting current-voltage curves, electrical losses, fuel production and several thermodynamic parameters of operation, i.e., efficiencies, fuel conversion, etc.. Typically, different level models are capable of predicting different data and the accuracy of the predictions usually drops as the scale of the model increases.

In this section the two most popular types of model are discussed, viz. micro- and macro- level models. System-level design is skipped due to its simplicity.

A macro-model simulation is based on Faraday's law, Butler-Volmer equation, Ohm's law and gas transport equations. Faraday's law relates the applied current to the flow of oxygen ions through the electrolyte. Ohm's law corresponds to the loss associated with the flow of oxygen ions in the electrodes on both sides of the electrolyte (often with assumed electrolyte thickness). Most commonly, it is assumed that electrodes have negligible electronic resistance, thus Ohm's law is limited to the electrolyte phase. The Butler-Volmer equation models

the increase in potential (overpotential) to initiate the reaction on each of the electrodes. Gas transport law links the drop in performance with concentration gradients across the electrode gas channel and the triple phase boundary (often with assumed thickness of electrode). The dusty gas model has been proved to be the most appropriate model and is most widely used to model the gas diffusion process. Other applied models are Fick's law and Maxwell-Stefan's law.

In a micro-model approach an attempt is taken to enhance the accuracy of the simulation by additional consideration of the cermet electrode microstructure. Cermets are composite materials made of metals and ceramics. They differ from the traditional metal electrodes by enhanced performance and a more complicated pattern of the reaction that occurs. A typical cermet electrode is Ni-YSZ or LSM-YSZ. It is impossible to accurately model electrode geometry as it is the result of many factors, i.e., materials fraction, production process, sintering procedure, etc. The micro-scale based approach was developed in order to better predict the performance of such electrodes. It is based on the statistic percolation theory describing the geometry of the electrode. The particle coordination number theory enables the effective values to be predicted of parameters such as conductivity, permeability, porosity, active surface area, etc. This technique utilizes the division of losses between the electrodes and the electrolyte, rather than activation, concentration and ohm loss.

Due to the compactness of the following work, all derivations are limited and the reader is introduced in main to the results and assumptions made.

3.2.1. Classical approach—macro-model

The most common way to model SOEC is by describing the limiting processes mentioned in the previous section through introducing the concept of overpotentials. This nomenclature came from electrochemistry and is actually entropy generation in thermodynamic terms, and can be categorized as: concentration overpotentials occurring in both electrodes, activation overpotentials occurring in both electrodes, Ohmic overpotentials occurring in the electrolyte and both electrodes (Figure 5).

Some researchers also considered offset overpoten-
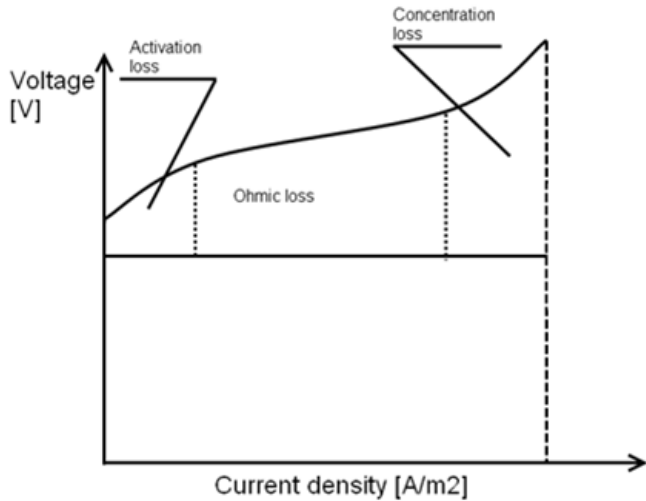
Figure 5: Typical shape of I-V curve for early cells with a clear distinction between different mechanisms of cell losses

tial, which is mainly due to contact resistance and is a constant. All other overpotentials are functions of operating conditions. In this approach, potential difference at the cell electrical terminal is expressed as (Eq. (7)):

$$
\begin{aligned}
E = E_0 &+ \eta_{\text{activation,anode}} + \eta_{\text{activation,cathode}} \\
&+ \eta_{\text{ohmic,anode}} + \eta_{\text{ohmic,cathode}} + \eta_{\text{ohmic,electrolyte}} \\
&+ \eta_{\text{concentration,anode}} + \eta_{\text{concentration,cathode}} + \eta_{\text{offset}}
\end{aligned} \tag{7}
$$

In the above equation E_0 is electrochemical potential or electromotive force, Greek etas correspond to the described overpotentials.

Open circuit voltage. In open circuit, electrochemical potential is the minimum potential difference required to split steam/carbon dioxide, or in SOFC mode as the maximum electromotive force obtained from converting fuel gases. It can be calculated by considering the minimum work concept of thermodynamics. For a control volume operating at steady state, the energy balance can be written as:

$$
0 = H_i - H_o + Q - W \tag{8}
$$

While the entropy balance can be written as:

$$
0 = S_i - S_o + \frac{Q}{T} + S_{gen} \tag{9}
$$

The concept of minimum work requires the assumption of reversible operation, hence S_{gen} is equal to zero and heat from equation (8) can be written as:

$$
Q = T (S_o - S_i) \tag{10}
$$

Now substituting eq. (10) into (8) and realizing that reversible system requires minimum work input to operate:

$$
0 = H_i - H_o + T (S_o - S_i) - W_{min} \tag{11}
$$

or using the definition of Gibbs potential:

$$
W_{min} = -\Delta G \tag{12}
$$

To calculate minimum work input to the system, the change in Gibbs free energy for the overall reaction is needed.

Minimum work can also be written as the integral of power consumption over a period of time:

$$
W_{min} = \int_0^t E(t) \cdot I(t) dt \tag{13}
$$

If the applied voltage is constant ($E(t) = const$), then equation (13) can be written as:

$$
W_{min} = E_0 \int_0^t I(t) dt = E_0 \cdot q \tag{14}
$$

The amount of charge transferred for 1 mole of fuel produced can be expressed as:

$$
q = zF \tag{15}
$$

Substituting (15) into (14) and back to (12) yields the basic electrochemistry relation:

$$
E_0 = \frac{-\Delta G}{zF} \tag{16}
$$

Gibbs free energy for ideal gas mixtures can be calculated using:

$$
G_i = G_i^0 + n_i RT \ln \left(\frac{p_i}{P_{std}} \right) \tag{17}
$$

where: n_i– number of moles of gas species i.

From the definition of chemical potential:

$$
\mu_i = \left(\frac{\partial G}{\partial n_i} \right)_{T=\text{const},P=\text{const},nj=\text{const}} \tag{18}
$$

One can obtain the relation between Gibbs free energy and chemical potential, i.e., $G = n\mu$, and thus equation (17) becomes:

$$G_i = n_i\mu_i^0 + n_iRT \ln\left(\frac{p_i}{P_{std}}\right) \quad (19)$$

If a reaction involving an ideal mixture is considered, the change in Gibbs free energy can be expressed as:

$$\Delta G = \sum G_i \text{ (products)} - \sum G_j \text{ (reactants)} \quad (20)$$

When the cell is fed with steam, the overall reaction follows:

$$H_2O \rightarrow H_2 + {}^1\!/_2 O_2 \quad (21)$$
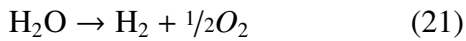
Using equations (19) and (20), the change in Gibbs free energy can be written as:

$$\Delta G = \mu_{H_2}^0 + RT \ln\left(\frac{p_{H_2}}{p_{std}}\right) + {}^1\!/_2\mu_{O_2}^0$$
$$+ {}^1\!/_2 RT \ln\left(\frac{p_{O_2}}{p_{std}}\right) - \mu_{H_2O}^0 - RT \ln\left(\frac{p_{H_2O}}{p_{std}}\right) \quad (22)$$

where:

$$\Delta G^0 = \mu_{H_2}^0 + {}^1\!/_2\mu_{O_2}^0 - \mu_{H_2O}^0 \quad (23)$$

Substituting equation (23) into (22) gives:

$$\Delta G = \Delta G^0 + RT \ln\left[\frac{p_{H_2}p_{O_2}^{1/2}}{p_{H_2O}p_{std}^{1/2}}\right] \quad (24)$$

Similar reasoning can be made for the reaction of carbon dioxide electrolysis and then substituting (24) into (16) and using the relation between partial pressure and mole fraction yields:

$$E_0 = \frac{-\Delta G_{f,H_2O}(T)}{2F} - \frac{RT}{2F} \ln\left[\left(\frac{y_{1,H_2O}}{y_{1,H_2}y_{O_2}^{1/2}}\right)\left(\frac{P}{P_{std}}\right)^{-1/2}\right] =$$
$$= \frac{-\Delta G_{f,CO_2}(T)}{2F} - \frac{RT}{2F} \ln\left[\left(\frac{y_{1,CO_2}}{y_{1,CO}y_{O_2}^{1/2}}\right)\left(\frac{P}{P_{std}}\right)^{-1/2}\right] \quad (25)$$

Note: Eq. (25) is only valid for a non-reacting gas mixture. Hence, for co-electrolysis the mixture must be brought to chemical equilibrium or quasi-equilibrium before applying the equation. The reaction occurring in a steam/carbon dioxide mixture

is a Water Gas Shift reaction (WGS) or a Reversed Water Gas Shift (RWGS) reaction, depending on the temperature of the mixture. The switching temperature between the two reactions is about 827°C, below which the former reaction dominates, i.e., the reaction will follow Eq. (26). Hydrogen and/or carbon monoxide produced from electrolysis are/is often re-circulated at the cathode to create a sufficient reducing environment in order to prevent the cathode materials from oxidation.

$$CO + H_2O \longleftrightarrow CO_2 + H_2 \quad (26)$$
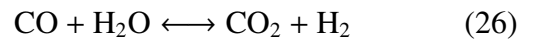
Activation overpotential. Activation overpotential on both electrodes is due to two phenomena. The first is chemical, i.e., the chemical equilibrium state of ions at the electrode-electrolyte interface. The second is electrical, i.e., overcoming of the electric field due to transfer of charged particles across the interface by ions. Thus, the free energy of activation has two constituents: the chemical energy of activation and the electrical contribution to it. Activation overpotential can be mitigated with increased temperature, active surface area and activity of catalyst used. Free activation energies of electrodes can be written as:

$$E^- = E_0^- + \alpha F \Delta\phi_e \quad (27)$$

and

$$E^+ = E_0^+ - (1 - \alpha) F \Delta\phi_e \quad (28)$$

where: $E_0^{+/-}$ is the chemical free energy, $\alpha F \Delta\phi$ is the electrical contribution, which amounts to lowering the energy barrier to electrode-to-ion transfer. Electronation is the process of transferring electrons from electrode to oxygen in order to form ions. Electronation current density can be expressed as follows:

$$\vec{j} = \frac{FkT}{h} c_m e^{-E_0^-/RT} e^{-\alpha F \Delta\phi_e/RT} \quad (29)$$

where: k is Boltzmann's constant, h is Planck's constant, F is Faraday's constant, R is Universal gas constant.

De-electronation is a process opposite to electronation and describes the process of transfer-

ring electrons from oxygen ions to electrode. De-electronation current density can be expressed as:

$$\overleftarrow{j} = \frac{FkT}{h} c_j e^{-E_0^+/RT} e^{(1-\alpha)F\Delta\phi_e/RT} \qquad (30)$$

At equilibrium, electronation and de-electronation current densities are equal, which represent the rate of reaction and are called exchange current density j_0. This value varies with temperature, electrode materials, gas composition, etc.
The difference between (29) and (30) represents net current flow. Defining the overpotential as the difference between non-equilibrium and equilibrium potentials

$$\eta = \Delta\phi - \Delta\phi_e \qquad (31)$$

one can arrive at the following expression:

$$j = \frac{FkT}{h} \left[\begin{array}{l} \left(c_j e^{-E_0^+/RT} e^{(1-\alpha)F\Delta\phi_e/RT} \right) e^{(1-\alpha)F\eta/RT} \\ - \left(c_m e^{-E_0^-/RT} e^{-\alpha F\Delta\phi_e/RT} \right) e^{-\alpha F\eta/RT} \end{array} \right] \qquad (32)$$

Utilizing the definition of exchange current density, a more compact expression can be obtained:

$$j = j_{0,i} \left[\exp\left(\frac{\alpha z F \eta_{\text{act},i}}{RT} \right) - \exp\left(-\frac{(1-\alpha) z F \eta_{\text{act},i}}{RT} \right) \right] \qquad (33)$$

This notion is called the Butler-Volmer equation. Often used in modeling is the assumption of a charge transfer coefficient $\alpha = 0.5$, then the following form can be used:

$$j = 2 j_{0,i} \sinh\left(\frac{F \eta_{\text{act},i}}{zRT} \right) \qquad (34)$$

Its linear approximation is given by:

$$\eta_{\text{act},i} = \frac{RT j}{zF j_{0,i}} \qquad (35)$$

where: $i = \{\text{anode, cathode}\}$, $j_{0,i}$ is exchange current density, which is a parameter linked to the kinetics of the electrode reaction. It has been established to obey the Arrhenius exponential dependence on temperature:

$$j_{0,i} = \gamma_i \exp\left(-\frac{E_{\text{act},i}}{RT} \right) \qquad (36)$$

Ohmic overpotential. Ohmic overpotential of the cell can be computed using equation (37)

$$\eta_{\text{Ohm}} = j\overline{R} \qquad (37)$$

where $\overline{R}$ is the combined ionic, electronic and contact resistance of the cell. Most commonly, only ionic resistance of the electrolyte is considered, other resistances are assumed to be orders of magnitude lower, thus negligible.

Concentration overpotential. Concentration overpotential is another key polarization of the cell especially at high current density. It is modeled in several different ways in the literature [40]. In general, it follows the mass transfer limitations of the porous electrodes. Concentration of species in the electrodes is same as the concentration in free stream only when no current is passing through the cell. Naturally, when current starts to pass through the electrodes, the concentration of fuel species at the interface, $c_{x=0}$, decreases from free stream value c^0. Due to the decrease in concentration, a respective voltage drop is present.

$$\eta_{\text{conc}} = \Delta\phi - \Delta\phi_e \qquad (38)$$

Applying the Nernst equation to the equilibrium state states:

$$\Delta\phi_e = \Delta\phi^0 + \frac{RT}{zF} \ln c^0 \qquad (39)$$

Respectively, when current flows through the cell Nernst potential can be written as:

$$\Delta\phi = \Delta\phi^0 + \frac{RT}{zF} \ln c_{x=0} \qquad (40)$$

Inserting equations (39) and (40) to (38) yields:

$$\eta_{\text{conc}} = \Delta\phi - \Delta\phi_e = \frac{RT}{zF} \ln \frac{c_{x=0}}{c^0} \qquad (41)$$

To calculate the concentration at interface, several methods can be applied: Fick's model, Stefan-Maxwell's model or Dusty Gas Model. A comparison of results using those models is presented in ref. [40].
In this section only the Dusty Gas Model (DGM) is highlighted since it has been proved to be the most appropriate for multi-component gas transport

in porous media [40]. The other models do not consider the effects of either multi-component flow or porous media. Nevertheless, it is important to note that simpler models suffice for many applications. According to DGM, transport of the species can be represented by Eqs. (42) and (43).

$$\frac{\varepsilon}{RT}\frac{\partial(p_i)}{\partial t} = -\nabla N_i + R_i \qquad (42)$$

$$\frac{N_i}{D_{i,k}^{\text{eff}}} + \sum_{j=1,j\neq i}^{n} \frac{y_j N_i - y_i N_j}{D_{ij}^{\text{eff}}} = -\frac{P}{RT}\frac{dy_i}{dx} \qquad (43)$$

Solving these equations yields partial pressures (concentrations) of involved gases at the triple phase boundary, i.e. the reaction site. Concentration loss for each of the electrodes is later calculated using Eqs. (44) and (45).

$$\eta_{\text{conc},i} = \frac{RT}{2F}\ln\left[\frac{p_{\text{H}_2}^{\text{I}}\left(p_{\text{O}_2}^{\text{I}}\right)^{1/2}}{p_{\text{H}_2\text{O}}^{\text{I}}}\right] \qquad (44)$$

$$\eta_{\text{conc},i} = \frac{RT}{2F}\ln\left[\frac{p_{\text{CO}}^{\text{I}}\left(p_{\text{O}_2}^{\text{I}}\right)^{1/2}}{p_{\text{CO}_2}^{\text{I}}}\right] \qquad (45)$$

Another approach to predicting concentration overpotential is by combining electrochemistry, mass transfer and boundary layer theory. This consideration results in introducing the limiting current density. It can be shown as:

$$\frac{j}{zF} = -D\left(\frac{dc}{dx}\right)_{x=0} = -D\left(\frac{c^0 - c_{x=0}}{\delta}\right) \qquad (46)$$

where: D is diffusivity.
Current density from the above equation is equal to limiting current density when $c_{x=0}$ equals zero:

$$\frac{j_{\text{L}}}{zF} = \lim_{c_{x=0}\to 0}\left[-D\left(\frac{c^0 - c_{x=0}}{\delta}\right)\right] = -D\frac{c^0}{\delta} \qquad (47)$$

Substituting (46) and (47) to (41) yields:

$$\eta_{\text{conc}} = \frac{RT}{zF}\ln\left(1 - \frac{j}{j_{\text{L}}}\right) \qquad (48)$$

Calculation of limiting current density follows from mass transfer analysis, and several formulae across the literature are used to derive the value.

3.2.2. Statistical approach—micro-modeling

When micro-modeling is considered, a slightly different approach is applied. Overpotentials are not divided between activation, concentration and Ohmic. Instead the balances of charge, Ohm's law and mass balance are evaluated for each electrode, while Ohm's law alone is considered for electrolyte. Therefore, one can write Ohm's law for the electronic conductor as:

$$\nabla\phi_{\text{el}} = \rho_{\text{e}}^{\text{eff}}j_{\text{e}} \qquad (49)$$

Similarly, for the ionic conductor:

$$\nabla\phi_{\text{i}} = \rho_{\text{i}}^{\text{eff}}j_{\text{i}} \qquad (50)$$

Since both electrodes are mixed conductors, charge balance must incorporate both ionic and electronic current densities.

$$\nabla j_{\text{e}} = -S_{\text{V}}j = -\nabla j_{\text{i}} \qquad (51)$$

j is the transfer current density calculated from the Butler-Volmer equation as in the classical model. S_{V} is the electrochemically active area per unit volume of the electrode, it is computed based on the statistical consideration.

$$S_{\text{V}} = \pi\sin^2\theta r_{\text{e}}^2 n_{\text{t}}n_{\text{e}}n_{\text{i}}\frac{Z_{\text{e}}Z_{\text{i}}}{6}P_{\text{e}}P_{\text{i}} \qquad (52)$$

For the definition of each symbol used above, readers are advised to refer to the nomenclature section at the end of this paper. The following formulae are based on the theory of the particle coordination number in the random packing of spheres and percolation theory, first used by Costamagna et al. [41]. The total number of particles per unit volume can be considered as:

$$n_{\text{t}} = \frac{1-\varepsilon}{(3/4)\,\pi r_{\text{e}}^3\left[n_{\text{e}} + (1-n_{\text{e}})\,(r_{\text{i}}/r_{\text{e}})^3\right]} \qquad (53)$$

Note that the mixture consists of ionic and electronic conductors, hence:

$$n_{\text{i}} = 1 - n_{\text{e}} \qquad (54)$$

The number of electronic conducting particles can be obtained from:

$$n_e = \frac{\Phi}{\Phi + (1 - \Phi)(r_i/r_e)^3} \qquad (55)$$

The coordination number for the electronic conductor can be expressed as:

$$Z_e = 3 + \frac{3}{n_e + (1 - n_e)(r_i/r_e)^2} \qquad (56)$$

Similarly, the coordination number for the ionic conductor can be written as:

$$Z_i = 3 + \frac{3(r_i/r_e)^2}{n_i + (1 - n_i)(r_i/r_e)^2} \qquad (57)$$

The probability for chain connectivity between the same types of particles can be calculated for electronic conductors and ionic conductors, respectively, from equations (58) and (59):

$$P_e = \left[1 - \left(\frac{4.236 - Z_{e-e}}{2.472}\right)^{2.5}\right]^{0.4} \qquad (58)$$

$$P_i = \left[1 - \left(\frac{4.236 - Z_{i-i}}{2.472}\right)^{2.5}\right]^{0.4} \qquad (59)$$

The average coordination number of electronic to electronic particles and ionic to ionic particles can be written as:

$$Z_{e-e} = \frac{6n_e}{n_e + (1 - n_e)(r_i/r_e)^2} \qquad (60)$$

$$Z_{i-i} = \frac{6n_i}{n_i + (1 - n_i)(r_i/r_e)^{-2}} \qquad (61)$$

Please note that most of the parameters in this model are difficult to obtain, thus often require mathematical fitting to experimental data.

Cathode model. Cathode overpotential can be expressed by:

$$\eta_c = \left(\phi_i^0 - \phi_e^0\right) - (\phi_i - \phi_e) \qquad (62)$$

Potentials can be evaluated using Ohm's law (eq. (49) and (50) for both types of conductors. Effective resistivity can be obtained by applying Eq. (63) for electronic and Eq. (64) for ionic conductors.

$$\rho_e^{\text{eff}} = \frac{\xi}{\Phi(1 - \varepsilon)\sigma_e} \qquad (63)$$

$$\rho_i^{\text{eff}} = \frac{\xi}{(1 - \Phi)(1 - \varepsilon)\sigma_i} \qquad (64)$$

The next step is to take the second derivative of Eq. (62), which results in the following expression:

$$\frac{d^2\eta_c}{dx^2} = S_V j_{0,c} \left(\rho_i^{\text{eff}} + \rho_e^{\text{eff}}\right) j \qquad (65)$$

where j is calculated according to Eq. (33). The boundary conditions are defined as follows:

$$\begin{cases} j_{i,c} = 0 & at \quad x = 0 \\ j_{e,c} = j_{\text{total}} & at \quad x = 0 \\ \frac{d\eta_c}{dx} = -\rho_{e,c}^{\text{eff}} j_{\text{total}} & at \quad x = 0 \\ j_{i,c} = j_{\text{total}} & at \quad x = \delta_c \\ j_{e,c} = 0 & at \quad x = \delta_c \\ \frac{d\eta_c}{dx} = -\rho_{i,c}^{\text{eff}} j_{\text{total}} & at \quad x = \delta_c \end{cases} \qquad (66)$$

The last step of derivation is related to the conservation of species. Since the DGM model was deemed to be most appropriate, only the final equation is provided.

$$\frac{d^2 y_i}{dx^2} + \frac{\beta}{D_{i,j}^{\text{eff}}} \left(\frac{1}{D_{i,k}^{\text{eff}}} + \frac{1 - \beta y_i}{D_{i,j}^{\text{eff}}}\right)^{-1} \left(\frac{dy_i}{dx}\right)^2 - \frac{S_V j R T}{2 F P} \left(\frac{1}{D_{i,k}^{\text{eff}}} + \frac{1 - \beta y_i}{D_{i,j}^{\text{eff}}}\right) = 0 \qquad (67)$$

Boundary conditions are defined as follows

$$\begin{cases} y_i = y_i^0 & at \quad x = 0 \\ \frac{dy_i}{dx} = -\frac{R T j_{\text{total}}}{2 F P} \left(\frac{1}{D_{i,k}^{\text{eff}}} + \frac{\sqrt{\frac{M_i}{M_j}} y_i}{D_{i,j}^{\text{eff}}}\right) & at \quad x = 0 \end{cases} \qquad (68)$$

Solving Eq. (65) and (67) with respect to the appropriate boundary conditions yields the total cathode overpotential.

2.2.2.2 Anode model

For the anode, similar reasoning can be applied to obtain an equation in same form as (65).

The difference is in the modeling of species conservation. Instead of using DGM to solve (42), Darcy's law can be applied. While the Dusty Gas Model is accurate for multicomponent diffusion in porous media, Darcy's law, derived from fluid flow in porous

media is simpler and accurate enough to model the flow of oxygen through air electrode (anode):

$$N_{O_2} = -\frac{P_{O_2} B_g}{RT\mu} \nabla p_{O_2} \tag{69}$$

The resulting governing equation is:

$$\frac{d^2 p_{O_2}}{dx^2} + \frac{1}{P_{O_2}} \left(\frac{dp_{O_2}}{dx}\right)^2 + \frac{S_V jRT\mu}{4FB_g P_{O_2}} = 0 \tag{70}$$

Appropriate boundary conditions are:

$$\begin{cases} y_{O_2} = y_{O_2}^0 & at \quad x = 0 \\ \frac{dp_{O_2}}{dx} = -\frac{RT j_{total}\mu}{2FP_{O_2} B_g} & at \quad x = 0 \end{cases} \tag{71}$$

Electrolyte model. Modeling of the electrolyte is the simplest part of the micro-model approach. Simple Ohm's law is used to evaluate the energy loss due to the passage of oxygen ions. A more detailed description of the process occurring in the electrolyte is described in ref. [42], but to the authors' best knowledge this approach was never utilized in modeling aimed at system or even cell design optimization.

More advanced models of electrolyte processes are employed in theoretical description of degradation phenomena called bubble formation [43]. Due to slow oxygen ion evolution within the electrode, high partial pressures of oxygen may develop with the electrolyte layer causing delaminations. Little is known as to the nature of this process.

4. Literature on modeling

Despite all the research on Solid Oxide Electrolysis Cells since the late Sixties [44–49] there are only a couple of dozen modeling papers available. The vast majority of them are from the 21st century. Although there are review papers on SOEC development [18], none specifically reviews modeling. In this work, an attempt is made to organize and review the efforts to date on SOEC modeling.

Research on SOEC modeling is associated with that of SOFC modeling, and is mostly on performance prediction and optimization, techno-economical assessment, and exploration for hydrogen or hydrocarbon fuel production. However, as discussed previously, the physical phenomena occurring in SOECs are different to those in SOFCs, hence changes in the approach are required.

4.1. Categories

For this work, the following tactics are used to organize the reviewed articles. Firstly, models are distinguished either in steady or transient state. Secondly, the two subgroups are further divided into micro-, macro or system levels models. Finally, models are classified by the number of dimensions considered in the study. A summary of the review articles is set out in Table 1.

4.2. Steady state models

Since SOEC technology is still non-commercial technology, most of the research done is with the assumption of steady state operation. This family of models allows the electrochemical, mechanical and thermal behavior of the cell, stack or system to be predicted.

4.2.1. System-level models

The choice of modeling papers is rather limited in this section, although the content is very interesting. A group from Idaho National Laboratory (INL), USA did thorough research on possibilities of producing syngas using nuclear energy. Another group investigated the use of geothermal energy.

The first paper to be reviewed here comes from a group in Hong Kong. Ni et al. in [50] reported energy and exergy analysis of a hydrogen production plant based on SOEC. The model was zero dimensional, steady state macro-level. Besides proposing the system architecture with heat recovery, they conducted a parametric study in order to optimize the plant. The model simulated the electrochemical and thermodynamic behavior of the plant, which did not include any pumps, or compressors, etc. The discussion in the paper suggested that coupling the plant with some unnamed industries to recover waste heat for application could lower hydrogen production costs. Although the plant itself required more heat energy at higher temperatures, the stack performed better and electrical energy demand was lower. At investigated conditions of 1073 K (800°C) and 5000 A/m^2, the largest exergy loss was associated with the stack, while the largest energy loss was

assigned to the heat exchangers. The authors found that current density, flow rate of steam and temperature have some impact on energy and exergy efficiency. They also attempted to explain the small difference in energy and exergy efficiency by stating that heat energy was only a small fraction of the whole energy delivered, and the quality of heat was high at elevated temperatures. They predicted energy efficiency as high as 70% and exergy efficiency of almost 80%.

The group from Idaho National Laboratory contributed largely to system-level analysis. Stoots et al. [51] presented a mathematical system level model of a stack with support from their in-house experimental data. The paper focused on high-temperature co-electrolysis aimed at producing syngas. Experiments and simulation temperature was set at 800°C. The model presented was only a minor feature of the paper and was based on a simplified electrochemical model, where the Nernst equation was used to predict Open Circuit Voltage (OCV), later cell potential was calculated based on the linear relation of voltage to current. An additional part of the model was on energy balance. Area Specific Resistance (ASR) was used in this model to calculate cell potential. ASR was a function of the operating temperature. To calculate the Nernst potential, the authors proposed bringing the reacting gas mixture to equilibrium and assumed the reaction to be Water Gas Shift Reaction. The authors proved a reasonable estimation of Open Circuit Voltage by using an equilibrated Nernst equation. The INL group also showed that co-electrolysis enhanced syngas production over a plain water gas shift reaction. Good agreement was shown between the predicted outlet composition variations and the experimentally observed ones.

In another paper by the same group [52], O'Brien et al. presented a parametric study of syngas production. Here they presented a complete system analysis using Aspen Plus Hysys. The model used was the same as in their previous paper, and the temperature remained unchanged too, but it was only one of the parameters for parametric study. They predicted efficiency of the plant to be as high as 48.3%. Estimation showed that for the production rate of 10 kg/s of syngas, a nuclear power plant with thermal capacity of 600 MW is required. The study analyzed reactor output temperature between 700 to 1000°C, which was far above commercial PWR or BWR, indicating gas cooled reactors (generation not yet developed). Cycle efficiency increased by half with a 300°C temperature rise. The authors also analyzed adiabatic and isothermal mode of operation. They also studied the impact of the assumed ASR value.

A group based in France investigated the possibility of hydrogen production using geothermal heat [53]. Again, a very simple linear model was used to evaluate the power response of an SOEC. The authors speculated the operating temperature of the cell to be between 700 and 900°C. Applying thermo-economic analysis of the plant, they arrived at feasibility with a geothermal heat source with a temperature as low as 230°C. At that temperature, an additional heater was required to supplement the heating. The electrolyzer was assumed to work around 950°C, when geothermal steam was supplied at 230°C.

Tri-generation system based on SOFC-SOEC coupling was modeled and analyzed in [54]. Perdikaris et al. analyzed planar SOEC and SOFC operating at 1173 K (900°C.) in a plant producing hydrogen, electricity and heat. Detailed plant modeling was provided. Models of SOEC and SOFC were linear and used the ASR concept. The authors also reported exergy analysis of the plant. In the system, the SOFC was fueled with methane. The electricity and heat produced were supplied to SOEC and other receivers. The SOEC then provided pure oxygen to burn off the exhaust gases from the SOFC. The carbon dioxide produced was later sent for storage. Predicted exergy efficiency of the system was about 45%.

Another analysis of a system for hydrogen production was produced by Gopalan et al. [55]. The system coupled the SOEC with a photovoltaic (PV) cell and solar heat exchangers. Solar radiation was split between the heat exchanger and PV cell to deliver electrical energy and heat energy to the SOEC stack. The study was divided into three subsections and utilized first law analysis to evaluate the temperatures and system efficiency after each step. Stack inlet temperature was 800°C. The model was based around thermodynamic considerations of temperatures of streams between three virtual steps of electrolysis: isothermal & adiabatic, adiabatic, and heat

loss. Operating voltage and current were the inputs to the model. The authors showed an efficiency increase if the cell operated above thermo-neutral voltage in a small stack. For a large stack, high efficiency was predicted for voltages around thermo-neutral. The model did not predict any significant efficiency changes subject to the variations of steam molar fraction at the inlet. The simulations presented in the paper were not validated. First law efficiency predicted was around 80–90%.

Another system level model reported was a collaborative effort between INL and NASA on a closed-loop atmosphere revitalization system [56]. Interestingly, NASA sponsored a similar study back in the Sixties and Seventies [47, 48]. The electrochemistry model presented in this paper is exactly the same as in other system level studies done at INL. The authors compared the effectiveness of co-electrolysis with other processes and concluded that combined co-electrolysis with hydrogenation was the most effective way to utilize carbon dioxide and achieve the highest overall performance. Models for all processes were prepared and run in Aspen Plus Hysys.

Iora et al. in [57] and [58] described and modeled a system for pure oxygen production based on coupling SOFC and SOEC technology. In the first reference, they provided a lumped model of the system allowing inputs of operating temperature, current, and inlet gas composition. The proposed model estimated the energy cost for oxygen production. In a later publication, the authors used a one-dimensional model which revealed a 60% overestimation of performance compared with that of the previous lumped model. The new model was able to predict the influence of operating temperature and its distribution, recirculation rate, current density, molar composition of gases on system efficiency and oxygen production capacity. The output of the model was energy consumption per kg unit of oxygen produced. Compared to the 0D, the 1D model required more complex, numerical solution of mass and energy balances and analytical solution of the electrochemistry model. The study also included modeling of cathode and anode channels as well as SOEC-SOFC interconnect.

Petipas et al [59] presented a dynamic behavior model of a pressurized hydrogen production system working with various loads. The authors predicted the initial performance of such system with an outstanding efficiency of 91%. However, they identified the problem of running the system under various loads. They proposed several technologies (i.e. electrical heating, electrode air sweep, modular operation) in order to allow operation at below 60% of the designed capacity. The electrolyzer model utilized in the study was a linear one. The authors attempted to increase the accuracy by iterative calculation of current based on area specific resistance, Nernst potential, cell power consumption and cell active area.

4.2.2. Macro-level models

In this category, macro-level models refer to the scale of electrodes or electrolyte thickness in tens of microns. This kind of model does not allow performance study of the electrode/electrolyte microstructure. However, they offer more parameters to be controlled than the system-level models.

The first article chosen for the review is perhaps the oldest paper, dating back to the late Sixties [49]. Spacil et al. described thermodynamics and cell characteristics in their paper. They considered an isothermal planar cell operating at 1000°C. The authors showed that the performance of the cell was dependent on the open circuit voltage, Ohmic resistance and mass transfer resistance. The authors provided thermodynamics derivations leading to open circuit voltage expression. They also analyzed the effect of the inlet gas steam fraction and steam conversion (fuel utilization) on OCV, showing that an increase in the initial fraction of steam and a decrease in steam reduction would lead to a decrease in open circuit voltage. The problem of heat management was identified and a solution proposed in the form of connecting cells in series and thus limiting the total heat loss. The authors stressed that this approach would increase the Ohmic loss.

To the authors' best knowledge, significant developments in the modeling of SOEC came only in this century. The first work chosen in the section came from Ni et al. [60] in 2006. This paper focused on modeling the concentration overpotentials of both SOEC and SOFC. The authors conducted a simulation of planar electrolyte-supported SOEC/SOFC operating at 800°C. They highlighted the differences in the mechanism of gas transport in porous electrodes.

Fick's model was used to obtain species partial pressures at electrode-electrolyte interface. The authors provided validation of I-V characteristics and steam molar fraction impact on cell potential at 2000 A/m². A parametric study was presented, analyzing the influence of steam molar fraction at inlet and thickness of electrodes on concentration loss. The results showed that performance increased with the increased steam molar fraction at the inlet and reduced electrode thicknesses. The simulation also showed that the design of the anode-supported cell would not significantly increase the concentration loss.

In [61], the same group conducted research on simulation and parametric study of the planar cell operated at 1000°C. They also performed comparative studies on electrolyte-, anode- and cathode-supported cells. Their model used Fick's law for concentration overpotential evaluation and a simplified Butler-Volmer equation with assumed symmetrical electrode polarization behavior for the activation overpotential calculation. The model was validated in the same manner as in their previous article [60]. Ni et al. showed that increasing temperature and steam composition might increase the energy efficiency of the cell. Superior performance was evident for the anode-supported cell and the authors recommended this cell configuration for the SOEC design. It is of note that the cathode-supported design is presently the most widely used.

The same group also conducted a more detailed parametric study on the hydrogen production system in [62]. The analyzed system and conditions are same as those in [61]. The authors showed that increasing the electrode porosity and pore size would reduce gas transport resistance. They also identified that elevated temperature enhances reaction kinetics and oxygen ions transport through the electrolyte. The authors proposed operating the stack at 1273 K (1000°C.) which is about the optimal point. An increased steam molar fraction would reduce Nernst potential and favor gas transportation. The impact of pressure was studied. It was shown that high pressure reduces concentration loss, but increases Nernst potential, thus 1 bar is proposed as the operating pressure for the anode-supported cell. However, elevated pressure was desirable for cathode supported cells operating at current density above 5000 A/m².

Another group based in France reported their work on SOEC modeling [63]. They performed 2D simulation on a planar type cathode-supported cell operating at 800°C. A multiphysics model, which included electrochemistry, thermodynamics and fluid mechanics, was solved using the COMSOL Multiphysics 3.4 platform. The DGM model was used to evaluate concentration losses. The authors investigated the results presented in [44], showing that at high current densities a one step Butler-Volmer equation was not accurate enough. Grondin et al. underlined the high sensitivity of the model to the parameters of the materials, e.g. exchange current densities, which in their model were fitted to values of 10^8 and 10^6 orders for anode and cathode, respectively, and in A/m². It is noteworthy that they assumed the electrode charge transfer reaction to occur symmetrically, whereas it has recently been speculated that this is a wrong assumption [64]. The two-dimensional model allowed them to investigate the influence of the gas feeding arrangement, which implicitly indicated that a better gas feeding design may increase the lifespan of the cell.

The same team, in [65], used their model to perform a parametric study on the hydrogen production unit. The authors developed an analytical solution for the DGM equations. The simulation was capable of predicting local temperature spatial distribution, heat fluxes, current densities, species concentrations and the overpotentials. To evaluate activation potentials, the authors used the Butler-Volmer equation with enhanced current density computation formulae incorporating the impact of gas species concentration. The study analyzed the influence of radiative heat loss to the environment, showing that this loss had a major impact on thermal equilibrium of the stack. The authors proposed operating the cells at thermo-neutral voltage to stabilize the stack temperature. Parametric study revealed the significance of anode activation losses. Although cathode activation losses were influenced by inlet gas composition, the absolute value did not vary significantly and the composition should be chosen according to other criteria, i.e. durability or system efficiency. Simulations showed the insignificance of anode concentration overpotentials. Cathode concentration overpotential was shown to be moderate for electrolyte-

supported design, and dramatically significant for the cathode-supported design. Addition of diluent to inlet gas composition increased the concentration overpotentials.

Another model chosen for this review reported a simulation of carbon dioxide electrolysis [66]. In the paper, Ni provided two models, one- and two-dimensional. The first model was an extension of models previously developed by Ni et al., while the second model offered additional thermal-fluid considerations. The analyzed cell was a cathode-supported planar design of very conservative elements thicknesses, operated at 900°C. The study showed the dominance of Ohmic loss (electrolyte thickness 100 microns) and the sluggish reaction of carbon dioxide electrolysis. Concentration loss at cathode was significant, due to the larger molecular weights of oxides of carbon. The author proposed increasing the operating pressure or porosity to decrease the concentration loss. Increasing the gas inlet velocity would enhance the performance of the SOEC by having more uniform gas distribution, but the authors did not investigate if increased gas velocity would influence gas conversion. Another investigated parameter was permeability of oxygen: varying this value between 10^{16} and 10^{13} [m^2] would not influence the concentration overpotential significantly.

Researchers from the USA reported another model for carbon dioxide electrolysis [67]. The aim of the paper was to demonstrate that gadolinium-doped ceria cathodes outperformed the classically used Ni-YSZ. The authors conducted experiments and later fitted the results into a CO-CO$_2$ exchange model. Do note that this model was not electrochemical. The experiments described in the article were on a half-cell design and AC impedance measurements were done and later modeled to verify the exchange mechanism. The authors extracted the vacancy diffusion coefficient, exchange rate and an undefined thermodynamic factor termed 'A'. The scientists found that almost the whole cathode was electrochemically active during electrolysis in the temperature range 700 to 950°C and oxygen partial pressures 10^{18} to 10^{14} atm.

A different study focused on cathodic process was undertaken by a group in France [68]. Grodin et al.

however, used an enhanced classical model applied to a half-cell. The researchers studied a Ni-cermet electrode by carrying out impedance and polarization measurements in the range of 700 to 900°C. The authors used two models for mass and charge transfer. At low steam molar fraction and high current densities, the use of a one rate-limiting step model, employing the Butler-Volmer equation, seemed to be inaccurate. A mechanism was proposed based on water molecule adsorption, which was equivalent to a two rate-limiting step model and the results were in good agreement with the experimental data.

Another type of model was used for co-electrolysis. Due to the complicated nature of the processes, the reported literature is very limited, there being only a few recent publications.

The first publication was contributed by Ni [69]. The author developed a 1D model of a cathode-supported planar SOEC operating at 800°C. In the simulation the author presented virtual division of the cell for the part responsible for electrolysis of steam and the part responsible for electrolysis of carbon dioxide. The author did not, however, comment on how to calculate cell equilibrium potential. Concentration loss was evaluated using the DGM model, and source term for species conservation as Reverse Water Gas Shift reaction (RWGS). Activation overpotentials were computed using the Tafel equation. Ni used the exchange current density values proposed in [70] for hydrogen and 40% of those for carbon dioxide, as observed from experiments. The model was validated with experimental data from the literature. The author showed that the rate of RWGS was positive and when the reaction was Water Gas Shift reaction, the rate became negative, depending on the temperature. It was proposed to use a gas composition equal to the average of those at the cathode surface and those predicted at the cathode-electrolyte interface as reference values for the RWGS reaction producing/consuming CO. The author showed that at the temperature of 873 K (600°C.) CO was produced, while at 1073 K it was consumed.

In another paper, the same author presented an extended 2D model of co-electrolysis [71]. The cell design assumptions were the same as in his previous article. The author investigated two reactions occurring in the reacting gas stream: the Reversed

Water-Gas Shift reaction and steam reforming reaction. The latter was shown to be not the preferred one in the analyzed conditions (873 K–1073 K). Apart from that, no changes were made to the model. The author studied the influence of inlet composition and operating pressure on the WGS and current densities for electrolysis, showing that the latter increased with the increased steam molar fraction. Similarly, increased operating voltage was observed with rising steam molar fraction.

A similar model to the one developed in [72] was employed to investigate the performance of the SOEC cell with delamination [73]. Jin and Xue simulated a delaminated oxygen electrode. The model was validated for two temperatures, 800 °C and 900 °C. Delamination was modeled by gaps in 2D geometry of the cell, and the simulation was solved using COMSOL Multiphysics 3.5a. The researchers studied the sensitivity of the cell to delamination in general and sensitivity to delamination occurring in different locations of the cell. The simulation revealed the high impact of gaps on performance. Delamination occurring in the center of the cell had the biggest influence, in contrast to delamination on the edges. A significant drop in performance occurred for both co- and counter-flow arrangements.

Another type of model is to be found in 3D simulations. To the authors' best knowledge these models have been developed only by the group from INL, USA.

Hawkes et al. [74] adopted the Fluent user-defined sub-routine developed for SOFC [75] and executed it for SOEC. The model was applied to a planar SOEC stack operating at 1103 K (830°C.). The model was capable of providing spatial distributions of temperature, Nernst potential, operating potential, gas composition, current density and hydrogen production rate. The model results were validated by in-house experimental results. The authors showed that for operation below thermo-neutral voltage, the electrolyte temperature would drop below the gas inlet temperature, with the minimum value being for 1.08 V. The opposite was observed for the above thermo-neutral voltage. Mean Nernst potentials increased with operating voltage and current density. Mean ASR values decreased with increasing current density. Hydrogen production varied linearly with current density, in accordance with Faraday's law.

In [76], an interesting comparison between 1D, 3D and experimental results was reported. O'Brien et al. compared their linear model with the CFD model and experimental results. The 1D model was capable of computing Nernst potential, cell voltage, gas outlet temperatures, extent of Ohmic heating and electrolyzer efficiency. Moreover, the 1D model was also capable of performing parametric study. One dimensional models have been shown to predict OCV correctly, and I-V characteristic slightly better than CFD and experimental data, making the model more conservative. Parametric study done on the cell revealed that lowering ASR and oxygen partial pressure at the anode offered higher efficiency. A similar effect would be achieved by elevating the temperature and lowering the pressure. The author showed that operating below thermoneutral voltage resulted in efficiencies exceeding 100%.

In [77], Dumortier et al. presented various modeling approaches for the simulation of heat transfer in SOEC. Their model could be implemented using COMSOL Multiphysics. The authors studied the influence of applied current density and inlet gases velocity on temperature distribution within the cell. They argued that temperature distribution and heat loss to the environment merely varied with applied current density and inlet gases velocity. Furthermore, the only temperature variation was inside the gas channels, not the PEN. Finally, they proposed an analytical means to calculate temperature inside each of the cell components.

4.2.3. Micro-level models

Micro-level SOEC modeling is very limited, but it is related to the work done on SOFC. Interested readers are recommended to study references [78–82].

The first paper chosen for review in this category is [42]. The authors in the following work focused on modeling ion-conducting electrolyte for SOFC and SOEC. The model was based on the relation between potential and concentrations of free electrons and electron holes. The impact of temperature, oxygen partial pressure, and electrolyte thickness on membrane permeability to oxygen was studied. Later, the influence of permeability was studied against the performance of SOC (Solid Oxide Cell). Various gas

mixtures were investigated at one side of the electrolyte.

Another paper on micro-modeling was directly linked with those developed for SOFC [83]. Ni et al. extended and adjusted their previous micro-model for SOFC [84] to make it applicable to SOEC. The 1D model was developed and validated for an electrolyte supported cell. Further parametric study, however, was done for an anode-supported cell with functionally graded electrodes (FGE), operating at 800°C. The study revealed that the majority of the reaction occurred in the vicinity (50 microns) of the electrode electrolyte interface. Increasing steam molar fraction and temperature enhanced the performance of the cell. Particle size of electrodes and porosity had optimal values which are traded off between gas transport resistance and volumetric density of the cell active surface area. FGM was found to be beneficial with smaller particle size close to the electrode-electrolyte interface, which allowed the electrochemically active area to be enhanced while maintaining good gas transport performance away from the interface.

Very recently, Grondin et al. published a paper [85] on an artificial neural network (ANN), which established relations based on a micro-model and later used for macro-modeling. The ANN used three inputs of overpotential, water concentration and hydrogen concentration to calculate current density of the cell. Data to "train" the network was simulated with the use of the model from [68]. The trained ANN created relations among current, electrode overpotential and inlet gas composition in the form of mixed hyperbolic and polynomial functions. These were input to COMSOL Multiphysics software, where a macro-level model was built. The authors claimed that the advantage of this model was the lower computational cost compared to that of the classical 3D model. They reported the numerical challenge to converge iteration in 10 hours on a 64 bit CPU 16 GB RAM Linux machine.

Another interesting paper was published by Shi et al. [86]. The authors investigated the elementary reaction of carbon dioxide reduction in SOEC. They developed a detailed one-dimensional model incorporating elementary heterogeneous reactions, electrochemical kinetics, electrode microstructure, mass transport and charge transfer phenomena. The proposed model was validated with experimental data and good agreement was obtained. Additionally, the authors identified the problem of carbon deposition at the electrode/electrolyte interface. They also performed several simulations to optimize electrode design.

4.3. Transient models

Transient, time-dependent, models of SOEC are not very popular. This might be explained by the stage of development of SOEC, which is still not commercial, hence studies on the dynamics of the cell are not essential yet. The usefulness of such models can be realized when safety features or control strategies are incorporated into the simulation of an SOEC stack. The latter was the subject of research at Imperial College London, UK. The group from Imperial College have published several papers [87–90] on transient modeling of an SOEC aimed at developing control strategies and studying the effects of operating conditions on the transient performance of an SOEC.

The model on transient behavior of SOEC developed by the group from Imperial College, appears to have been based on the model they developed earlier for SOFC [91, 92].

In [87] Udugawa et al. prepared a dynamic model of a cathode-supported planar SOEC stack operating at 800°C. Although the equations presented contained time derivatives, only steady-state analysis was performed. They studied the influence of operating current and temperature on the irreversible losses, showing that increased temperature and decreased current density could reduce the losses. They also showed that the major contribution to losses was due to activation overpotential. Less electricity consumption per square meter was required to produce a unit volume of hydrogen as compared with low-temperature electrolysis. Dependence of current distribution on cell temperature was identified as a possible issue, so a proper control strategy could be applied to prolong the lifespan of the stack.

Reference [88] provided with temperature control strategy for issue described in [87]. Air flow was introduced on the anode side of the cell in order to equalize the temperature distribution along the cell. Dynamic response of the cell with and without air

flow control was analyzed showing that the strategy might be successful. It was predicted that the control strategy would be capable of returning the stack to design temperature in less than 800 seconds for both exo- and endo-thermic mode of operations, while being tried with steep current changes

In reference [89] Udagawa et al. performed simulations on the same model as in their previous papers, showing additional results on introducing air stream at the anode side. Decreasing the concentration of oxygen on air electrode lowers the theoretical Nernst potential required to start cell operation. The authors showed low efficacy of the control strategy if the cell was operated at thermo-neutral voltage and they suggested omitting this mode of operation.

None of the above models [87–89] were validated with experimental measurements. Only the latest article [90] from this group provided a section on model validation.

In [90] Cai et al. presented, again, the same model as in their three previous articles and employed it to simulate stack behavior at various temperatures, inlet gas compositions and steam utilization factors. They identified temperature and current density as the most influential factors for stack performance. In this study, they proposed to operate the stack at the temperature of 1073 K (800°C) and current density of 10000 A/m^2. Under the prescribed conditions the dynamic response of the cell temperature to varying current was the most stable. Investigation of the inlet gas compositions showed the steam molar fraction had a negligible influence on stack voltage, but a significant influence on temperature. Cai et al. also proposed to use air electrode to fuel electrode flow ratio of 7 to maintain constant temperature along the stack.

The purpose of their study was to address issues that might arise from coupling the SOEC with an intermittent energy source, i.e. wind or solar energy. The authors also underlined that results may change when system-level study is introduced, due to the additional energy required for pumping air to the anode.

In all of the above mentioned papers, a set of differential equations had to be solved. The authors used gPROMS Model Builder 3.0.3 [93] in their study.

Another hydrogen electrode-supported planar SOEC transient model was developed by Jin et al. [72].

Their efforts were focused on modeling of a cell in switching mode of SOFC/SOEC. The proposed model used the symmetrical Butler-Volmer equation for the activation loss, Maxwell-Stefan's law for the concentration loss and Ohm's law for the Ohmic loss. Gas flow was modeled by the Navier-Stokes equation in gas channels and by the Brinkman equation in the porous electrodes. The model was validated with in-house experimental data. The aim of the model was to investigate dynamic response of the cell under switching conditions. The authors demonstrated that the distribution of the ionic potential and of hydrogen, oxygen and steam species flips when the mode was changed. Electronic potential, however, exhibits different behavior. For the hydrogen electrode, the potential stayed at zero voltage, while for the oxygen electrode it switched from low in SOFC mode to high in SOEC mode. This model was solved by COMSOL Multiphysics 3.5.

The above summarizes the most typical research activities on the modeling of Solid Oxide Cells. The later part of this review is devoted to more unusual models and materials.

4.4. Different models

The first paper chosen for review in this category is devoted to the co-ionic electrolyte cell [94]. Demin et al. described operation of an SOEC based electrolyte allowing for the flow of oxygen anions and hydrogen cations, when subjected to an electric field. The model was based on species fluxes balance and thermodynamic considerations for electromotive forces for both of the transported ions. The partial pressures of gases at the input and output were assumed. Then, initial values of fluxes were guessed, and electromotive forces and current densities at the initial point were calculated. This routine was run in a certain computational domain and when convergence was achieved for the output values, iterations would stop. This approach yielded higher current densities and more uniform parameter distribution within the cell.

Another model under review was on electrolyte [95]. Jacobsen and Mogensen analyzed the course of partial pressure of oxygen and electric potentials in SOEC. To express this, they adopted Galvani and Volta potentials. Electron holes and ions transport

were investigated. A mechanism was proposed for the delamination that occurred in the anodes of the SOEC. The authors showed that this phenomenon would not occur in an SOFC.

A completely different approach to SOFC modeling was shown in [96]. Although the model was developed to simulate an SOFC, it can be easily customized for an SOEC. Bessler et al. showed the possibility of modeling based on an elementary-kinetic description of electrochemistry rather than the use of overpotentials. Other highlights of the model were as follows: the model did not use the Nernst equation, thus it could be applied to non-equilibrated mixtures. The model used the Navier-Stokes equation and Fick's law to model transport phenomena. It incorporated time dependent derivatives, allowing for transient calculations. It also allowed for quasi-3D spatial computations. Instead of showing contributions of a different loss mechanism to overall performance loss, this model showed the contribution of each element of the cell. Predicted values for OCV were in much better agreement than for those from a classical model. The authors manipulated the model with an assumption of equilibrated gases and arrived with the Nernst equation, proving the enhanced generality of their model. Nevertheless, this model suffered from more dependence on intrinsic parameters, like elementary reaction kinetic parameters, etc. The model showed good potential for application with genetic programming to extract basic information from elementary reactions in an SOC.

At the end of this paper, we would like to feature our own contribution to modeling. Due to overwhelming interest in SOEC technology over the past few years, the need has grown for accurate calculations of SOEC systems and for simulation of large amounts of experimentally unavailable data. The authors prepared cross level model of SOEC allowing for investigation of how cell microstructural design can affect system operations and how the SOEC system operates in conditions departing from those experimentally investigated. As a result, a 0-dimentional SOEC cross-level model was developed [64] and used in conjunction with a power plant [97]. In the first publication we performed energy and exergy analysis of an SOEC working as a CO_2 mitigation device. The system is combined with a conventional power plant. In a non-optimized system a 67% reduction of CO_2 was achieved with 50% thermal efficiency. Our model enabled calculation of the activation potential with charge transfer coefficient $\alpha \neq 0.5$ and included simple modeling of reaction kinetics. Parameters for the model were fitted and validated with in-house and literature experimental data, showing good agreement. In the second paper we analyzed a similar system of electrolyzer combined with a traditional power plant. We looked at the influence of exhaust gas recycling, temperature and gas feed molar flux on efficiency, current density, voltage, steam and carbon dioxide conversion, carbon dioxide conversion performance and electricity consumption. A modified layout of the system was proposed with a temperature control module and heat recovery. The list of plant included compressors working as fans, an electric heater and heat exchangers. Electricity-to-syngas efficiency achieved was 46.2%. Carbon dioxide mitigation performance of 2.57 mol CO_2/kWh was achieved at 500°C. A set of recommendations was presented for incorporation of an SOEC into a power plant.

5. Concluding remarks

SOEC technology has attracted a lot of attention in recent years due to its potential to provide sustainability of development, security of energy resources and technical advantages over other electrolysis technologies, i.e. high efficiency and possibility of direct reduction of CO_2 emissions. Efforts have been put into developing long lasting materials and exploring possible applications [98, 99]. Options including fossil fuel recycling, curbing CO_2 emissions, harnessing renewable energy sources and producing high quality fuels and oxygen make this technology extremely interesting for science, business and the environment [100, 101].

Despite all the on-going research, there is still a lack of understanding of the fundamental reaction mechanism of co-electrolysis. At issue is whether CO_2 is electrolyzed or chemically converted through the water gas shift reaction. Another research gap is on understanding and quantifying the degradation mechanism. There are only a few experimental studies on the long term degradation of an SOEC, while some

reported an increase in performance over time [102]. There is no confirmation to date on what contributes to cell degradation or on what to do to extend the lifespan of an SOEC [103]. Next, we would like to draw attention to the main shortcoming of almost every model in this review. Very few of them were thoroughly validated with experimental results. In most cases, validation was limited to only one I-V curve or was even absent. Moreover, most authors took the approach to simply adapt the SOFC modeling techniques by changing the polarization direction. However, it is well understood that the processes occurring in SOECs are different from those in SOFCs, hence a thorough analysis of the applicability of SOFC methods is necessary. In some cases, the authors claimed a more complex activation process, therefore stated that the Butler-Volmer equation was invalid [85]. For others, activation polarization was simply assumed to be a linear equation [71] relating voltage to current. We prefer the assumption of favoring one direction of charge transfer (charge transfer coefficient different from 0.5, i.e., non-symmetrical electronation) [64]. Lastly, there are limited resources in terms of modeling study of off-design conditions or dynamic behavior of the cell resulting from combining with intermittent energy sources, i.e. wind or solar energy used to drive the electrolysis. It is anticipated that more advanced research will soon appear, addressing the issues listed above and exploring new possible uses of the technology.

Acknowledgements

References

[1] W. Nicholson, A. Carlisle, Account of the new electrical or galvanic apparatus of alessandro volta and experiments performed with the same, Journal of Natural Philosophy, Chemistry and Arts 4 (1801) 179–187.

[2] K. Zeng, D. Zhang, Recent progress in alkaline water electrolysis for hydrogen production and applications, Progress in Energy and Combustion Science 36 (2010) 307–326.

[3] M. Faraday, Experimental Researches in Electricity, Richard and John Edward Taylor, London, 1849.

[4] W. H. Nernst, Die elektromotorische wirksamkeit der ionen, Zeitschrif fuer physikalische Chemie, Stoechiometrie und Verwandtschaftslehre 4 (1889) 129–181.

[5] W. Ostwald, Elektrochemie: Ihre Geschichte und Lehre, Veit, Leipzig, 1896.

[6] R. Hill, M. D. Archer, Photoelectrochemical cells – a review of progress in the past 10 years, Journal of photochemistry and photobiology. A, Chemistry 51 (1990) 45–54.

[7] S. Z. Baykara, Experimental solar water thermolysis, International Journal of Hydrogen Energy 29 (2004) 1459–1469.

[8] A. Steinfeld, Solar thermochemical production of hydrogen – a review, Solar Energy 78 (2005) 603–615.

[9] I. K. Kapdan, F. Kargi, Bio-hydrogen production from waste materials, Enzyme and Microbial Technology 38 (2006) 569–582.

[10] M. Ni, D. Y. C. Leung, M. K. H. Leung, A review on reforming bio-ethanol for hydrogen production, International Journal of Hydrogen Energy 32 (2007) 3238–3247.

[11] M. N. Manage, D. Hodgson, N. Milligan, S. J. R. Simons, D. J. L. Brett, A techno-economic appraisal of hydrogen generation and the case for solid oxide electrolyser cells, International Journal of Hydrogen Energy 36 (2011) 5782–5796.

[12] R. W. Coughlin, M. Farooque, Hydrogen production from coal, water and electrons, Nature 279 (1979) 301–303.

[13] F. Bidrawn, G. Kim, G. Corre, J. T. S. Irvine, J. M. Vohs, Efficient reduction of co_2 in a solid oxide electrolyzer, Electrochemical and Solid-State Letters 11 (2008) B167–B170.

[14] G. Gahleitner, Hydrogen from renewable electricity: An international review of power-to-gas pilot plants for stationary applications, International Journal of Hydrogen Energy 38 (2013) 2039–2061.

[15] M. Carmo, D. L. Fritz, J. Mergel, D. Stolten, A comprehensive review on pem water electrolysis, International Journal of Hydrogen Energy 38 (12) (2013) 4901–4934.

[16] T. Riedel, M. Claeys, H. Schulz, G. Schaub, S.-S. Nam, K.-W. Jun, M.-J. Choi, G. Kishan, K.-W. Lee, Comparative study of fischer-tropsch synthesis wit h_2 /co and h_2 /co$_2$ syngas using fe- and co-based catalysts, Applied Catalysis A: General 186 (1999) 201–213.

[17] C. R. Graves, Recycling co2 into sustainable hydrocarbon fuels: Electrolysis of co2 and h2o, Ph.D. thesis, Columbia University (2012).

[18] C. Schlitzberger, N. O. Brinkmeier, R. Leithner, Co2 capture in sofc by vapor condensation and ch4 production in soec storing excess electricity, Chemical Engineering Technology 35 (2012) 440–444.

Table 1: Summary and comparison of review papers

Number of dimensions	Considered structure	Inputs	Outputs	Contribution	Reference
0D	System	Current density, Temperature, Waste heat recovery	Electrical potential, Plant energy and exergy efficiency, Operational cost, Hydrogen production cost, Energy consumption, Steam conversion, Irreversible losses (overpotentials)	Energy and exergy analysis of the SOEC based system for production of hydrogen	[50]
0D	System (cell + stack modeling)	Current density, Temperature, Inlet gas composition	Electrical potential, Outlet gas composition, Stack temperature	Analysis of syngas production by co-electrolysis validated with in-house experiments.	[51]
0D	System	Current density, Temperature, Inlet gas composition, Syngas production rate, Operating voltage, Steam/CO_2 utilization	Electrical potential, System efficiency, Cell temperature	Parametric study of a large scale plant based on a nuclear powered SOEC to produce syngas	[52]
0D	System	Current density, Temperature of the geothermal source,	Electrical potential, Hydrogen cost	Parametric study of a large scale plant based on geothermal powered SOEC to hydrogen	[53]
0D	System	Current density, Temperature,	Electrical potential, Exergy efficiency	Energy and exergy analysis of tri-generation system based on SOEC-SOFC	[54]
0D	System	Operating voltage, Temperature, Steam utilization, Heat exchanger area	Energy efficiency	Energy and exergy analysis of tri-generation system based on SOEC-SOFC	[55]

0D	System	Current density, Temperature, Inlet gas composition, Steam/CO_2 utilization	Electrical potential, System efficiency, Cell temperature	Analysis of technologies for atmosphere revitalization for extra-terrestrial applications	[56]
0D and 2D	System	Current density, Temperature, Inlet gas composition, utilization	Electrical potential, System efficiency,	Analysis of technology for oxygen production based on SOFC-SOEC coupling,	[57]
0D	System	Current density, Temperature, Cell active area, Area Specific resistance	Electrical potential, System efficiency, cell temperature,	Analysis of a system under various loading conditions	[59]
0D	Cell and stack	Temperature, Steam utilization, Steam inlet concentration,	OCV, Electrical potential	Early thermodynamic analysis of water dissociation resulted in recommendation for connecting cells in series	[49]
0D	Cell	Temperature, Current, Cell microstructure	Electrical potential, Irreversible losses (overpotentials)	Concentration overpotential evaluation for SOEC and SOFC with prediction of gases partial pressures at electrode-electrolyte interface	[60]
0D	Cell, three types of support: cathode, anode electrode, microstructure, Gas composition	Temperature, Current, Cell composition	Electrical potential, Irreversible losses (overpotentials)	Electrochemical model of steam electrolysis, three different cell designs investigated	[61]
0D	Cell	Temperature, Current, Cell microstructure, Gas composition	Electrical potential, Irreversible losses (overpotentials)	Parametric study of hydrogen production based on SOEC	[62]
2D	Cell	Temperature, Current, Gas composition	Electrical potential distribution, Gas composition distribution, Temperature distribution	Identification of Butler-Volmer equation inaccuracy at specific operation conditions	[63]
2D and 1D	Cell	Temperature, Current, Cell composition	Electrical potential distribution, Irreversible losses (overpotentials), Gas composition distribution, Electrolyte temperature	Electrochemical model and parametric study of carbon dioxide electrolysis,	[66]

Dim.	Scale	Inputs	Outputs	Description	Ref.
0D	Cell	Temperature, Oxygen partial pressure, Electrode geometry	Vacancy diffusion coefficient, Exchange rate, Thermodynamic factor A, Utilization thickness of electrode	CO-CO$_2$ exchange model to predict impedance measurements	[67]
1D	Half cell	Temperature, Current	Irreversible loss (overpotential)	Water molecule adsorption model was proposed to simulate irreversible loss instead of Butler-Volmer equation	[68]
1D	Cell	Temperature, Current, Cell geometry, Inlet gas composition	Electric potential, gas composition distribution	Model of co-electrolysis incorporating water gas shift reaction	[69]
2D	Cell	Temperature, Current, Cell geometry, Inlet gas composition	Electric potential, Gas composition distribution, Temperature distribution, Rate of reactions distribution	Model of co-electrolysis incorporating water gas shift reaction, reversed methanation reaction and reforming reaction	[71]
2D	Cell	Temperature, Current, Cell geometry	Electric potential, Gas composition distribution	Model of SOEC with delaminations	[73]
3D	Cell	Temperature, Current, Cell geometry	Electric potential, Gas composition distribution, Cell efficiency, Cell temperature distribution	Sub-routine for SOEC modeling in Fluent	[74]
3D and 1D	Cell	Temperature, Current, Cell geometry	Electric potential, Gas composition, Cell efficiency, Cell temperature distribution	Comparison between 1D linear and 3D model results	[76]
2D	Cell	Inlet gases velocity, Current, Cell geometry	Temperature distribution	New technique for modeling heat transfer within PEN, Means for analytical determination of cell component's temperature	[77]
1D	Cell	Temperature, Current, Cell geometry, Oxygen partial pressure	Electric potential, Outlet gas composition, Electrolyte efficiency, Rate of oxygen permeation	Electrolyte micro-model for SEOC and SOFC	[42]
1D	Cell	Temperature, Current, Cell geometry, Cell microstructure	Electric potential, Gas composition distribution within the cell, Ionic and electronic current densities distribution, Irreversible losses (overpotentials)	Micro-level model of SOEC for hydrogen production, introduction of Functionally Graded Materials (FGM)	[84]

2D Cell	Temperature, Current, Cell geometry,	Electric potential distribution, Gas composition distribution within the cell, Cathodic overpotential distribution, Temperature distribution	Micro-level model was developed to train ANN. Developed relations for electrodes overpotentials were used for 2D modeling	[85]
1D Cell	Temperature, Current, Cell geometry, Elementary reaction kinetics	Electric potential distribution, Gas composition distribution within the cell,	Proposed elementary reaction kinetics for CO$_2$/CO electrolysis, optimization of electrodes for carbon dioxide electrolysis	[86]
1D Stack	Current density, Temperature, Inlet composition, Stack geometry	Electrical potential, Irreversible losses (overpotentials), Electricity consumption per unit of hydrogen produced,	Identification of issues with temperature control during dynamic operation	[87]
1D Stack	Current density, Temperature, Inlet composition, Stack geometry	Electrical potential, Irreversible losses (overpotentials), Electricity consumption per unit of hydrogen produced,	Control strategy for dynamic operation proposed, Response to step changes in current density analyzed	[88]
1D Stack	Current density, Temperature, Inlet composition, Stack geometry	Electrical potential, Irreversible losses (overpotentials), Electricity consumption per unit of hydrogen produced,	Operation near thermo-neutral voltage should be avoided, due to low controllability of stack temperature at this point	[89]
1D Stack	Current density, Temperature, Inlet composition, Stack geometry	Electrical potential, Irreversible losses (overpotentials),	Control strategy for SOEC used to produce hydrogen from intermittent energy sources	[90]
2D Cell	Current density, Temperature, Stack geometry, Steam molar fractions, steam utilisation	Electrical potential, Hydrogen and Oxygen distribution inside the cell, electronic and ionic potential distribution within the cell	Behavior of the cell during switching between SOEC and SOFC mode	[72]
1D Cell	Temperature, Current, Cell geometry,	Electric potential distribution, Gas composition distribution within the cell	Model of co-ionic SOEC cell	[85]
1D Cell	Temperature, Cell geometry, Oxygen partial pressure, Current,	Electric potential distribution, Oxygen partial pressure distribution	Thermodynamic model of oxygen partial pressure and electric potentials in SOEC	[95]

Quasi-3D	Cell	Temperature, Cell geometry, Current,	Electric potential distribution, Gas composition distribution,	New framework for modeling based on elementary kinetic description of electrochemistry, physical representation of potential steps, quasi-3D multi scale modeling, transient formulation	[96]
0D	Cross-level	Temperature, current density, cell materials and geometry, pressure, gas composition,	Energy efficiency, exergy efficiency, output gas composition, feedstock chemicals conversion, power plant emissions reduction	Considered kinetics of electrochemical reaction, allowed accurate predictions of feedstock conversion for co-electrolysis	[64]
0D	Cross-level	Temperature, current density, cell materials and geometry, pressure, gas composition, exhaust gas recycling, gas molar flux	Energy efficiency, output gas composition, feedstock chemicals conversion, power plant emissions reduction	Investigated detail impact of cell design parameters on system performance	[97]

[19] M. Ni, M. K. H. Leung, D. Y. C. Leung, Technological development of hydrogen production of solid oxide electrolyzer cell (soec), International Journal of Hydrogen Energy 33 (2008) 2337–2354.

[20] M. A. Laguna-Bercero, Recent advances in high temperature electrolysis using solid oxide fuel cells: A review, Journal of Power Sources 203 (2012) 4–16.

[21] F. Kargi, Microbiological coal desulphurization, Enzyme and Microbial Technology 4 (1982) 13–19.

[22] A. Blaszczuk, W. Nowak, S. Jagodzik, Effects of operating conditions on denox system efficiency in supercritical circulating fluidized bed boiler, Journal of Power Technologies 93 (1) (2013) 1–8.

[23] A. Sciubidlo, W. Nowak, Novel sorbents for flue gas purification, Journal of Power Technologies 92 (2) (2012) 115–126.

[24] G. Wiciak, J. Kotowicz, Experimental stand for co2 membrane separation, Journal of Power Technologies 91 (4) (2011) 171–178.

[25] S. Pascala, R. Socolow, Stabilization wedges: Solving the climate problem for the next 50 years with current technologies, Science 305 (2004) 968–972.

[26] M. C. Sheppard, R. H. Socolow, Sustaining fossil fuel use in a carbon-constrained world by rapid commercialization of carbon capture and sequestration, American Institute of Chemical Engineers 53 (2007) 3022–3028.

[27] I. Dincer, Renewable energy and sustainable development: a crucial review, Renewable and Sustainable Energy Reviews 4 (2000) 157–175.

[28] W. M. Budzianowski, I. Chasiak, Expansion of the biogas fuelled power plants in germany during the 2001 – 2010 decade: Main sustainable conclusions for poland, Journal of Power Technologies 91 (2) (2011) 102–113.

[29] P. Krawczyk, K. Badyda, Modeling of thermal and flow processes in a solar waste-water sludge dryer with supplementary heat supply from external sources, Journal of Power Technologies 91 (1) (2011) 37–40.

[30] P. Moriarty, D. Honnery, Intermittent renewable energy: The only future source of hydrogen?, International Journal of Hydrogen Energy 32 (2007) 1616–1624.

[31] A. Vojvodic, J. K. Norskov, Optimizing perovskites for the water-splitting reaction, Science 334 (2011) 1355–1356.

[32] E. D. Wachsmann, K. T. Lee, Lowering the temperature of solid oxide fuel cells, Science 334 (2011) 935–939.

[33] J. Milewski, K. Swirski, Modeling the sofc behaviours by artificial neural network, International Journal of Hydrogen Energy 34 (2009) 5546–5553.

[34] International Energy Agency, Key world energy statistics (2010).

[35] I. Ridjan, B. Van Mathiesen, D. Connolly, N. Duic, The feasibility of synthetic fuels in renewable energy systems, Energy 57 (2013) 76–84.

[36] National Research Council and National Academy of Engineering, The National Academies Press, Washington, D.C. USA, The Hydrogen Economy. Opportunities,

[37] W. E. Winsche, K. C. Hoffman, F. J. Salzano, Hydrogen: Its future role in the nation's energy economy, Science 180 (1973) 1325–1332.

[38] J. Milewski, K. Swirski, M. Santarelli, P. Leone, Advanced Methods of Solid Oxide Fuel Cell Modeling, Springer Verlag, 2011.

[39] S. Kakac, A. Pramuanjaroenkij, X. Y. Zhou, A review of numerical modeling of solid oxide fuel cells, International journal of hydrogen energy 32 (2007) 761–786.

[40] R. Suwanwarangkul, E. Croiset, M. W. Fowler, P. L. Douglas, E. Entchev, M. A. Douglas, Performance comparison of fick's, dusty-gas and stefan-maxwell models to predict the concentration overpotential of a sofc anode, Journal of Power Sources 122 (2003) 9–18.

[41] P. Costamagna, P. Costa, V. Antonucci, Micro-modeling of solid oxide fuel cell electrodes, Electrochimica Acta 43 (1998) 375–394.

[42] S. H. Chan, X. J. Chen, K. A. Khor, An electrolyte model for ceramic oxygen generator and solid oxide fuel cell, Journal of Power Sources 111 (2002) 320–328.

[43] O. Comets, P. Voorhees, Equilibrium nucleation calculation, available in: Barnett S. A.: Potential Performance of SOECs.
URL http://indico.conferences.dtu.dk/getFile.py/access?resId=15&materialId=slides&confId=131

[44] E. J. L. Schouler, M. Kleitz, E. Forest, E. Fernandez, P. Fabry, Overpotential of h2-h2o, ni/ysz electrodes in steam electrolyzers, Solid State Ionics 5 (1981) 559–562.

[45] A. O. Isenberg, Energy conversion via solid oxide electrolyte electrochemical cells at high temperatures, Solid State Ionics 3–4 (1981) 431–437.

[46] W. Doenitz, R. Schmidberger, E. Steinheil, R. Streicher, Hydrogen production by high temperature electrolysis of water vapor, International Journal of Hydrogen Energy 5 (1980) 55–63.

[47] J. Weissbart, W. H. Smart, Study of electrolytic dissociation of co2-h2o using a solid oxide electrolyte, Tech. rep., Lockheed Missiles & Space Company (1967).

[48] L. Elikan, J. P. Morris, C. K. Wu, Development of solid electrolyte carbon dioxide and water reduction system for oxygen recovery, Tech. rep., Westinghouse Electric Corporation (1972).

[49] H. S. Spacil, C. S. Tedmon Jr., Electrochemical dissociation of water vapor in solid oxide electrolyte cells: I. thermodynamics and cell characteristics, Journal of Electrochemical Society 116 (1969) 1618–1626.

[50] M. Ni, M. K. H. Leung, D. Y. C. Leung, Energy and exergy analysis of hydrogen production by solid oxide steam electrolyzer plant, International Journal of Hydrogen Energy 32 (2007) 4648–4660.

[51] C. M. Stoots, J. E. O'Brien, J. S. Herring, J. J. Hartvigsen, Syngas production via high-temperature co-electrolysis of steam and carbon dioxide, Journal of

Fuel Cell Science and Technology 6 (2009) 011014–1–011014–12.

[52] J. E. O'Brien, M. G. Mc Kellar, C. M. Stoots, J. S. Herring, G. L. Hawkes, Parametric study of large-scale production of syngas via high-temperature co-electrolysis, International Journal of Hydrogen Energy 34 (2009) 4216–4226.

[53] J. Sigurvinsson, C. Mansilla, P. Lovera, F. Werkoff, Can high temperature steam electrolysis function with geothermal heat, International Journal of Hydrogen Energy 32 (2007) 1174–1182.

[54] N. Perdikaris, K. D. Panopoulos, P. Hofmann, S. Spyrakis, E. Kakaras, Design and exergetic analysis of a novel carbon free tri-generation system for hydrogen, power and heat production from natural gas, based on combined solid oxide fuel and electrolyser cells, International Journal of Hydrogen Energy 35 (2010) 2446–2456.

[55] S. Gopalan, M. Mosleh, J. J. Hartvigsen, R. D. Mc Connell, Analysis of self-sustaining recuperative solid oxide electrolysis system, Journal of Power Sources 185 (2008) 1328–1333.

[56] M. G. Mc Kellar, M. S. Sohal, C. M. Stoots, L. Mulloth, B. Luna, M. B. Abney, Mathematical analysis of high-temperature co-electrolysis of co2 and o2 production in a closed-loop atmosphere revitalization system, Tech. rep., INL (2010).

[57] P. Iora, P. Chiesa, High efficiency process for the production of pure oxygen based on solid oxide fuel cell – solid oxide electrolyzer technology, Journal of Power Sources 190 (2009) 408–416.

[58] P. Iora, M. A. A. Taher, P. Chiesa, N. P. Brandon, A one dimensional solid oxide electrolyzer-fuel cell stack model and its application to the analysis of a high efficiency system for oxygen production, Chemical Engineering Science 80 (2012) 293–305.

[59] F. Petipas, A. Brisse, C. Bouallou, Model-based behaviour of a high temperature electrolyser system operated at various loads, Journal of Power Sources 239 (2013) 584–595.

[60] M. Ni, M. K. H. Leung, D. Y. C. Leung, A modeling study on concentration overpotentials of a reversible solid oxide fuel cell, Journal of Power Sources 163 (2006) 460–466.

[61] M. Ni, M. K. H. Leung, D. Y. C. Leung, An electrochemical model of a solid oxide steam electrolyzer for hydrogen production, Chemical Engineering Technology 29 (2006) 636–642.

[62] M. Ni, M. K. H. Leung, D. Y. C. Leung, Parametric study of solid oxide steam electrolyzer for hydrogen production, International Journal of Hydrogen Energy 32 (2007) 2305–2313.

[63] D. Grondin, J. Deseure, A. Brisse, M. Zahid, P. Ozil, Simulation of a high temperature electrolyzer, Journal of Applied Electrochemistry 40 (2010) 933–941.

[64] J. P. Stempien, O. L. Ding, Q. Sun, S. H. Chan, Energy and exergy analysis of solid oxide electrolyzer cell (soec) working as co2 mitigation device, International Journal of Hydrogen Energy 37 (2012) 14518–14527.

[65] J. Laurencin, D. Kane, G. Delette, J. Deseure, F. Lefebvre-Joud, Modeling of solid oxide steam electrolyser: Impact of the operating conditions on hydrogen production, Journal of Power Sources 196 (2011) 2080–2093.

[66] M. Ni, Modeling of a solid oxide electrolysis cell for carbon dioxide electrolysis, Chemical Engineering Journal 164 (2010) 246–254.

[67] R. D. Green, C.-C. Liu, S. B. Adler, Carbon dioxide reduction on gadolinia-doped ceria cathodes, Solid State Ionics 179 (2008) 647–660.

[68] D. Grondin, J. Deseure, P. Ozil, J.-P. Chabriat, B. Grondin-Perez, A. Brisse, Computing approach of cathodic process within solid oxide electrolysis cell: Experiments and continuum model validation, Journal of Power Sources 196 (2011) 9561–9567.

[69] M. Ni, An electrochemical model for syngas production by co-electrolysis of h2o and co2, Journal of Power Sources 202 (2012) 209–216.

[70] S. H. Chan, K. A. Khor, Z. T. Xia, A complete polarization model of a solid oxide fuel cell and its sensitivity to the change of cell component thickness, Journal of Power Sources 93 (2001) 130–140.

[71] M. Ni, 2d thermal modeling of a solid oxide electrolyzer cell (soec) for syngas production by h2o/co2 co-electrolysis, International Journal of Hydrogen Energy 37 (8) (2012) 6389–6399.

[72] X. Jin, X. Xue, Mathematical modeling analysis of regenerative solid oxide fuel cells in switching mode conditions, Journal of Power Sources 195 (2010) 6652–6658.

[73] X. Jin, X. Xue, Computational fluid dynamics analysis of solid oxide electrolysis cells with delaminations, International Journal of Hydrogen Energy 35 (2010) 7321–7328.

[74] G. L. Hawkes, C. M. O'Brien, J. E. nad Stoots, J. S. Herring, M. Shahnam, Cfd model of a planar solid oxide electrolysis cell for hydrogen production from nuclear energy, in: The 11th International Topical Meeting on Nuclear Reactor Thermal-Hydraulics (NURETH-11), 2005.

[75] M. Prinkey, M. Shahnam, W. A. Rogers, SOFC FLUENT Model Theory Guide and User Manual, Release Version 1.0, FLUENT, Inc. (2004).

[76] J. E. O'Brien, C. M. Stoots, G. L. Hawkes, Comparison of a one-dimensional model of a high-temperature solid-oxide electrolysis stack with cfd and experimental results, in: 2005 ASME International Mechanical Engineering Congress and Exposition, 2005.

[77] M. Dumortier, J. Sanchez, M. Keddam, O. Lacroix, Energy transport inside a three-phase electrode and application to a proton-conducting solid oxide electrolysis cell, International Journal of Hydrogen Energy 38

(2013) 2610–2623.

[78] P. Costamagana, P. Costa, V. Antonucci, Micro-modeling of solid oxide fuel cell electrodes, Electrochimica Acta 43 (1998) 375–394.

[79] X. Deng, A. Petric, Geometrical modeling of the triple-phase-boundary in solid oxide fuel cells, Journal of Power Sources 140 (2005) 297–303.

[80] S. H. Chan, X. J. Chen, K. A. Khor, Cathode micromodel of solid oxide fuel cell, Journal of Electrochemical Society 151 (2004) A164–A172.

[81] S. H. Chan, Z. T. Xia, Anode micro model of solid oxide fuel cell, Journal of The Electrochemical Society 148 (2001) A388–A394.

[82] S. Sohn, J. H. Nam, D. H. Jeon, C.-J. Kim, A micro/macroscale model for intermediate temperature solid oxide fuel cells with prescribed fully-developed axial velocity profiles in gas channels, International Journal of Hydrogen Energy 35 (2010) 11890–11907.

[83] M. Ni, M. K. H. Leung, D. Y. C. Leung, Mathematical modeling of the coupled transport and electrochemical reactions in solid oxide steam electrolyzer for hydrogen production, Electrochimica Acta 52 (2007) 6707–6718.

[84] M. Ni, M. K. H. Leung, D. Y. C. Leung, Parametric study of solid oxide fuel cell performance, Energy conversion & management 48 (2007) 1525–1535.

[85] D. Grondin, J. Deseure, P. Ozil, J.-P. Chabriat, B. Grondin-Perez, A. Brisse, Solid oxide electrolysis cell 3d simulation using artificial neural network for cathodic process description, Chemical Engineering Research and Design 91 (1) (2013) 134–140.

[86] Y. Shi, Y. Luo, N. Cai, J. Qian, S. Wang, W. Li, H. Wang, Experimental characterization and modeling of the electrochemical reduction of co_2 in solid oxide electrolysis cells, Electrochimica Acta 88 (2013) 644–653.

[87] J. Udagawa, P. Aguiar, N. P. Brandon, Hydrogen production through steam electrolysis: Model-based steady state performance of a cathode-supported intermediate temperature solid oxide electrolysis cell, Journal of Power Sources 166 (2007) 127–136.

[88] J. Udagawa, P. Aguiar, N. P. Brandon, Hydrogen production through steam electrolysis: model-based dynamic behaviour of a cathode-supported intermediate temperature solid oxide electrolysis cell, Journal of Power Sources 180 (2008) 46–55.

[89] J. Udagawa, P. Aguiar, N. P. Brandon, Hydrogen production through steam electrolysis: Control strategies for a cathode-supported intermediate temperature solid oxide electrolysis cell, Journal of Power Sources 180 (2008) 354–364.

[90] Q. Cai, E. Luna-Oritz, C. S. Adjiman, N. P. Brandon, The effects of operating conditions on the performance of a solid oxide steam electrolyser: A model-based study, Fuel Cells 6 (2010) 1114–1128.

[91] P. Aguiar, C. S. Adjiman, N. P. Brandon, Anode-supported intermediate-temperature direct internal reforming solid oxide fuel cell: model-based steady-state performance, Journal of Power Sources 138 (2004) 120–136.

[92] P. Aguiar, C. S. Adjiman, N. P. Brandon, Anode-supported intermediate-temperature direct internal reforming solid oxide fuel cell: Ii model-based dynamic performance and control, Journal of Power Sources 147 (2005) 136–147.

[93] Process Systems Enterprise Ltd., gPROMS Introductory User Guide (2002).

[94] A. Demin, E. Gorbova, P. Tsiakaras, High temperature electrolyzer based on solid oxide co-ionic electrolyte: A theoretical model, Journal of Power Sources 171 (2007) 205–211.

[95] T. Jacobsen, M. Mogensen, The course of oxygen partial pressure and electric potentials across an oxide electrolyte cell, ECS Transactions 13 (2008) 259–273.

[96] W. G. Bessler, S. Gewies, M. Vogler, A new framework for physically based modeling of solid oxide fuel cells, Electrochimica Acta 53 (2007) 1782–1800.

[97] J. P. Stempien, Q. Sun, S. H. Chan, Performance of power generation extension system based on solid-oxide electrolyzer cells under various design conditions, Energy 55 (2013) 647–657.

[98] F. Tietz, D. Sebold, A. Brisse, J. Schefold, Degradation phenomena in a solid oxide electrolysis cell after 9000 h of operation, Journal of Power Sources 223 (2013) 129–135.

[99] J. Kim, H.-I. Ji, H. P. Dasari, D. Shin, H. Song, J.-H. Lee, B.-K. Kim, H.-J. Je, H.-W. Lee, K. J. Yoon, Degradation mechanism of electrolyte and air electrode in solid oxide electrolysis cells operating at high polarization, International Journal of Hydrogen Energy 38 (2013) 1225–1235.

[100] H. Zhang, S. Su, X. Chen, G. Lin, J. Chen, Configuration design and performance optimum analysis of a solar-driven high temperature steam electrolysis system for hydrogen production, International Journal of Hydrogen Energy 38 (11) (2013) 4298–4307.

[101] A. Patyk, T. M. Bachmann, A. Brisse, Life cycle assessment of h_2 generation with high temperature electrolysis, International Journal of Hydrogen Energy 38 (2013) 3865–3880.

[102] X. Zhang, J. E. O'Brien, R. C. O'Brien, J. J. Hartvigsen, G. Tao, G. K. Housley, Improved durability of soec stacks for high temperature electrolysis, International Journal of Hydrogen Energy 38 (2013) 20–28.

[103] S. D. Ebbesen, J. Hogh, K. A. Nielsem, J. U. Nielsen, M. Mogensen, Durable soc stacks for production of hydrogen and synthesis gas by high temperature electrolysis, International Journal of Hydrogen Energy 36 (2011) 7363–7373.

Nomenclature

α Charge transfer coefficient

β $1 - N_{H_2}/N_{H_2O}$

ΔG_f Change in standard molar Gibbs' free energy of reaction, J

δ Thickness, m

$\dot{h}$ Electron hole

η Overpotential, V

γ Pre-exponential factor, A m^{-2}

μ Dynamic viscosity of oxygen, kg m^{-1}s^{-1}

$\overline{R}$ Resistance, Ω

Φ Volumetric fraction of electronic conductors in porous electrode

ϕ Potential, V

π Pi number, 3.14

ρ Resistivity, Ω m

σ Conductivity or average atom size, S m^{-1}

θ Contact angle between ionic and electronic conducting particles, rad

ε Porosity or molar exergy, J mol^{-1}

ξ Tortuosity, A

A Area, m^2

B_g Permeability, m^2

c^0 Concentration of species in the free stream

$c_{j,m}$ Concentration of ions crossing the electrode-electrolyte interface

$c_{x=0}$ Concentration of species at the electrode-electrolyte interface

CO Carbon monoxide

CO_2 Carbon dioxide

D Diameter or diffusivity, μ m or m s^{-2}

$D_{i,j}$ Binary diffusion coefficient, ms^{-2}

$D_{i,k}$ Knudsen diffusion coefficient, ms^{-2}

E Cell potential difference, V

e^- Electron

E_0 Nernst Voltage, V

E_{act} Activation energy, J mol^{-1}

F Faraday constant 96485.3365, C mol^{-1}

h Oxygen vacancy in electrolyte lattice

h Specific enthalpy or Planck's constant 6.626068×10^{-34}, J mol^{-1} or m^2 kg^{-1}s^{-1}

H_2O Water

H_2 Hydrogen

H_i Enthalpy in, J

H_o Enthalpy out, J

j Current density, A m^{-2}

j_0 Exchange current density, A m^{-2}

j_L Limiting current density, A m^{-2}

k Boltzmann's constant $1.3806503 \times 10^{-23}$, m^{2}kg s^{-2} K^{-1}

n Number of moles

n_e Number fraction of electronic conductors

N_i Mol flux of species i, mol s^{-1}

n_i Number fraction of ionic conductors or number of moles of species i

n_t Total number of particles per unit volume

O_2 Oxygen

$O_2^=$ Oxygen ion

O_o^x Oxygen atom adsorbed in electrolyte lattice

P Pressure, bar

P_e Probability of electronic particles connecting to porous media

P_i Probability of ionic particles connecting to porous media

p_i Partial pressure of i-th species, bar

Q Heat, J

q Charge transferred per 1 mole of fuel, C mol^{-1}

R Universal gas constant, J mol^{-1}K^{-1}

r_e Radius of electronic particle, μm

R_i Creation or destruction of species i, mol cm^{-3}s^{-1}

r_i Radius of ionic particle, μm

S_i Entropy in, J

S_o Entropy out, J

T Temperature, K

W Work, J

X Ratio of length of grain contact neck to grain size

y_i Molar fraction of species i

z Number of electrons transferred per reaction

Z_{e-e} Average coordination number of electronic particles to electronic particles

Z_e Average coordination number of electronic conductors

Z_{i-i} Average coordination number of ionic particles to ionic particles

Z_i Average coordination number of ionic conductors

0   In the free stream

eff   Effective

I   At the electrode-electrolyte interface